GE PANAMETRICS
Waltham, MA 02453

TITLE

Proton and Electron Calibration Report

GOES NO/PQ MAGPD Telescope

Engineer 11/23/04	Configuration Control for D.C. 11/23/04			
Product Assurance 11/23/04	Program Physicist 11/23/04			
Program Manager 11/23/04	Program Engineer 11/23/04	SIZE A	DRAWING NUMBER GOESN-ENG-029	REV -
				SHEET 1 OF 41

RELEASE AND REVISION RECORD

Rev.	Authority	Description	Release	
			Date	Approved
-	F. Hanser	Initial Release	11/23/04	

TABLE OF CONTENTS

Section	Title	Page
1.0	**INTRODUCTION**	**6**
1.1	Purpose	6
1.2	Reference Documents	6
1.3	Acronym List	7
2.0	**GEOMETRIC FACTOR DEFINITION AND MEASUREMENT**	**8**
2.1	Geometric Factor Definition	8
2.2	Experimental Measurement of the Geometric Factor	9
2.3	Equipment Setup	12
3.0	**DATA ANALYSIS AND RESULTS**	**16**
3.1	Measured Detector Areas	16
3.1.1	1MPi Proton Channel Measured Areas for Protons at GSFC	16
3.1.2	1MPi Proton Channel Measured Areas for Electrons at MIT	23
3.2	Measured Geometric Factors	29
3.2.1	Proton Geometric Factors	29
3.2.2	Electron Geometric Factors	34
3.3	Comparison of Measured and Calculated Responses	35
3.2.1	Calculated Responses	35
3.3.2	Proton Responses	36
3.3.3	Electron Responses	41
4.0	**SUMMARY AND CONCLUSIONS**	**41**

LIST OF FIGURES

Figure	Title	Page
Figure 2-1.	MAGPD Telescope Design and FOV	8
Figure 2-2.	Electron Shielding Magnetic Field Orientation in the MAGPD Telescopes	11
Figure 2-3.	Calibration Configuration at MIT Van de Graaff	13
Figure 2-4.	Electronics Configuration at MIT Van de Graaff	14
Figure 3-1.	Angular Response of 1MP1 and 1MP2 at 111.3 keV	22
Figure 3-2.	Angular Response of 1MP1, 1MP2 and 1MP3 at 122.5 keV	22
Figure 3-3.	Vertical Angular Response of 1MP1, 1MP2 and 1MP3 for 770 keV Electrons	27
Figure 3-4.	Horizontal Angular Response of 1MP1, 1MP2 and 1MP3 for 770 keV Electrons	28
Figure 3-5.	MAGPD Gf(E) Plots for GSFC Proton Calibration Data	32
Figure 3-6.	MAGPD Area(0 deg, E) Plots for GSFC Proton Calibration Data	32
Figure 3-7.	MAGPD and MEPED Gf(E) Plots for Proton Calibration Data	33
Figure 3-8.	MAGPD and MEPED Area(0 deg, E) Plots for Proton Calibration Data	33
Figure 3-9.	MAGPD Gf(E) Plots for MIT Electron Calibration Data	34
Figure 3-10.	MAGPD Telescope Energy Loss Curves	36
Figure 3-11.	Measured Relative 1MPi A(0 deg) Values as a Function of Proton Energy	37
Figure 3-12.	Recommended and Measured MP1 Gf(E) Values as a Function of Proton Energy	38
Figure 3-13.	Recommended and Measured MP2 Gf(E) Values as a Function of Proton Energy	39
Figure 3-14.	Recommended and Measured MP3 Gf(E) Values as a Function of Proton Energy	39
Figure 3-15.	Recommended and Measured MP4 Gf(E) Values as a Function of Proton Energy	40
Figure 3-16.	Recommended and Measured MP5 Gf(E) Values as a Function of Proton Energy	40

LIST OF TABLES

Table	Title	Page
Table 1-1.	Referenced Documents	6
Table 1-2.	List of Acronyms	7
Table 2-1.	Solid Angle Factor ($\Delta\Omega_i$) Values for GSFC Proton Calibration	10
Table 2-2.	Solid Angle Factor ($\Delta\Omega_i$) Values for MIT Electron Calibration	11
Table 3-1.	Measured 1MPi Detection Areas in cm^2 for 69.1 keV Protons	16
Table 3-2.	Measured 1MPi Detection Areas in cm^2 for 74.2 keV Protons	16
Table 3-3.	Measured 1MPi Detection Areas in cm^2 for 79.3 keV Protons	17
Table 3-4.	Measured 1MPi Detection Areas in cm^2 for 85.0 keV Protons	17
Table 3-5.	Measured 1MPi Detection Areas in cm^2 for 97.8 keV Protons	17
Table 3-6.	Measured 1MPi Detection Areas in cm^2 for 106.9 keV Protons	18
Table 3-7.	Measured 1MPi Detection Areas in cm^2 for 111.3 keV Protons	18
Table 3-8.	Measured 1MPi Detection Areas in cm^2 for 116.7 keV Protons	18
Table 3-9.	Measured 1MPi Detection Areas in cm^2 for 122.5 keV Protons	19
Table 3-10.	Measured 1MPi Detection Areas in cm^2 for 157 keV Protons	19
Table 3-11.	Measured 1MPi Detection Areas in cm^2 for 200 keV Protons	19
Table 3-12.	Measured 1MPi Detection Areas in cm^2 for 218 keV Protons	20
Table 3-13.	Measured 1MPi Detection Areas in cm^2 for 241 keV Protons	20
Table 3-14.	Measured 1MPi Detection Areas in cm^2 for 274 keV Protons	20
Table 3-15.	Measured 1MPi Detection Areas in cm^2 for 521 keV Protons	21
Table 3-16.	Additional Measured 1MPi 0 Degree Detection Areas in cm^2 for Protons	21
Table 3-17.	Measured 1MPi Detection Areas in cm^2 for 770 keV Electrons (Horizontal)	23
Table 3-18.	Measured 1MPi Detection Areas in cm^2 for 802 keV Electrons (Horizontal)	23
Table 3-19.	Measured 1MPi Detection Areas in cm^2 for 1140 keV Electrons (Horizontal)	24
Table 3-20.	Measured 1MPi Detection Areas in cm^2 for 1620 keV Electrons (Horizontal)	24
Table 3-21.	Measured 1MPi Detection Areas in cm^2 for 2100 keV Electrons (Horizontal)	24
Table 3-22.	Measured 1MPi Detection Areas in cm^2 for 2600 keV Electrons (Horizontal)	25
Table 3-23.	Measured 1MPi Detection Areas in cm^2 for 770 keV Electrons (Vertical)	25
Table 3-24.	Measured 1MPi Detection Areas in cm^2 for 870 keV Electrons (Vertical)	25
Table 3-25.	Measured 1MPi Detection Areas in cm^2 for 1140 keV Electrons (Vertical)	26
Table 3-26.	Measured 1MPi Detection Areas in cm^2 for 1620 keV Electrons (Vertical)	26
Table 3-27.	Measured 1MPi Detection Areas in cm^2 for 2100 keV Electrons (Vertical)	26
Table 3-28.	Measured 1MPi Detection Areas in cm^2 for 2600 keV Electrons (Vertical)	27
Table 3-29.	Measured 1MPi and Total Geometric Factors for Protons at GSFC	29
Table 3-30.	Measured 1MPi and Total Area(0 degrees) for Protons at GSFC	30
Table 3-31.	PM TIROS/NOAA MEPED 0 deg Telescope Proton Calibrations at GSFC	31
Table 3-32.	PM TIROS/NOAA MEPED 90 deg Telescope Proton Calibrations at GSFC	31
Table 3-33.	Measured 1MPi and Total Geometric Factors for Electrons at MIT	34
Table 3-34.	Calculated Proton and Electron MAGPD Channel Energies	35
Table 3-35.	Measured MAGPD Proton Channel Transition Energies	37
Table 3-36.	Recommended MAGPD Proton Channel Gf(E) Values for Protons	38

1.0 INTRODUCTION

1.1 Purpose

This report presents the results of the particle calibration of the EM MAGPD Telescope No. 1 performed using the (high energy) electron beam from the MIT Van de Graaff (VdeG) accelerator in Building N-10 at MIT, Cambridge, MA; the (low energy) proton beam from the Cockroft-Walton accelerator at the GSFC Radiation Effects Laboratory in Greenbelt, MD; and the (high energy) proton VdeG accelerator at the GSFC Radiation Effects Laboratory in Greenbelt, MD. The data have been reduced to the geometric factors necessary to convert the nMP1 through nMP5 (n = 1 through 9, for the MAGPD telescopes) proton channel telemetry data into proton fluxes, and to correct the data for electron flux contamination using the MAGED and EPEAD electron flux data. The measured area vs. angle data are also given, to provide information on the angular responses of the MAGPD proton channels.

1.2 Reference Documents

Table 1-1 lists the documents referenced in this report. The first is the test procedure used to acquire the data, while the second and third are the Calibration Report and Accelerator Calibration Test Procedure for a nearly identical proton telescope design used in the TIROS/NOAA spacecraft SEM-2 MEPED. The last three references are the tabulated stopping powers used to obtain the calculated responses, and to calculate corrections to the beam energies measured by the monitor detectors.

Table 1-1. Referenced Documents

Ref. #	Report Number	Date	Title
1	GOESN-RTP-140, Rev. -	Run Aug. – Sept., 2004	Procedure, Calibration, MAGPD
2	TIR-ENG-116, Rev. -	July 27, 1994	TIROS SEM-2 PM MEPED/SN 0010 Calibration Report
3	TIR-RTP-156, Rev. -	May 8, 1991	Test Procedure, MEPED Accelerator Calibration
4	NASA SP-3012	1964	Tables of Energy Losses and Ranges of Electrons and Positrons; M. J. Berger and S. M. Seltzer
5	NASA SP-3036	1966	Additional Stopping Power and Range Tables for Protons, Mesons, and Electrons; M. J. Berger and S. M. Seltzer
6	Atomic Data and Nuclear Data Tables	Vol. 27, Nos. 4/5, July/September 1982	Proton Range-Energy Tables, 1 keV – 10 GeV, Part 2, Elements; J. F. Janni

1.3 Acronym List

The acronyms used in this report are listed in Table 1-2.

Table 1-2. List of Acronyms

Acronym	Definition
1MPi	Proton channel "i" in proton telescope 1 of the MAGPD ("i" = 1 to 5)
nMPi	Proton channel "i" in proton telescope n of the MAGPD ("i" = 1 to 5; n = 1 to 9)
EM	Engineering Model
EPEAD	Energetic Proton, Electron and Alpha Detector
EPS	Energetic particle Sensor
FOV	Field-of-View
GOES NOPQ	Geostationary Operational Environmental Satellite N, O, P, and Q
GSFC	Goddard Space Flight Center
IFC	In Flight Calibration
MAGED	Magnetospheric Electron Detector
MAGPD	Magnetospheric Proton Detector
MEPED	Medium Energy Electron and Proton Detector
MIT	Massachusetts Institute of Technology
MF	Major Frame
Mf	Minor Frame
NOAA	National Oceanic and Atmospheric Administration
PM	Protoflight Model
SEM	Space Environment Monitor
SEM-2	Space Environment Monitor 2 (TIROS/NOAA spacecraft)
SSD	Solid State Detector
TIROS	Television Infra-Red Observational Satellite
VdeG	Van de Graaff Accelerator

2.0 GEOMETRIC FACTOR DEFINITION AND MEASUREMENT

2.1 Geometric Factor Definition

The geometric factors of the 1MP1 through 1MP5 proton channels are defined by an integral of the detection area over solid angle. A detection area of $A(E,\Omega)$ cm^2 for protons of energy E MeV and angle Ω, the geometric factor G(E) is given by

$$G(E) = \int A(E,\Omega)\, d\Omega \ cm^2\text{-sr} \qquad (2.1)$$

where $d\Omega = (\sin\theta)\, d\theta\, d\varphi$, with θ the elevation angle and φ the azimuth angle. For an isotropic proton flux $J(E)$ $p/(cm^2\text{-s-sr})$ the channel count rate is given by

$$C_{ei} = \int J(E)\, G(E)\, dE \ s^{-1} \qquad (2.2)$$

For a proton flux where there is also an angle dependence, the channel count rate is given by

$$C_{el} = \int J(E,\Omega)\, A(E,\Omega)\, dE\, d\Omega \ s^{-1} \qquad (2.3)$$

For normal conditions the geometric factor (2.1) is used, with the count rate given by (2.2).

The design of the MAGPD telescopes is shown in Figure 2-1, with all nine (9) telescopes being identical. The telescope FOV is cylindrically symmetric, with a full width of 30 degrees. Each telescope has an electron shielding magnet set to reduce the electron flux below several hundred keV.

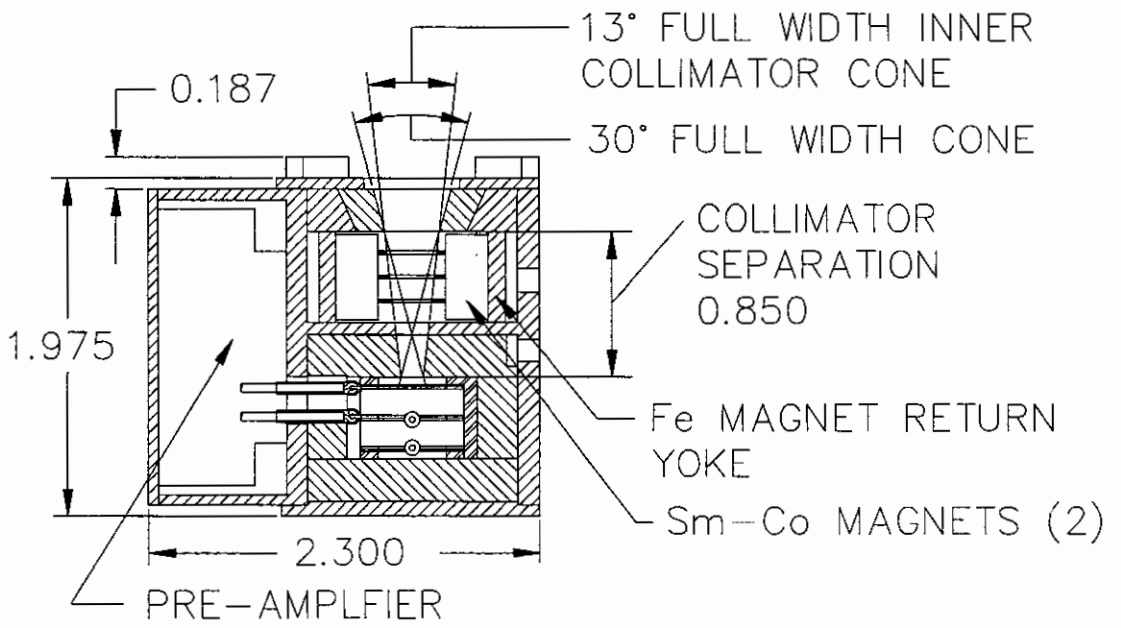

Figure 2-1. MAGPD Telescope Design and FOV

2.2 Experimental Measurement of the Geometric Factor .

The experimental measurement of G(E) is done by measuring the angular response A(E,Ω) at several angles. The integrated geometric factor is then calculated by a numerical sum

$$G(E) = \sum_i A(E,\Omega_i)\,\Delta\Omega_i \qquad (2.4)$$

where

$$\Delta\Omega_i = 2\pi \times (\cos\theta_{1i} - \cos\theta_{2i}) \qquad (2.5)$$

with θ being the polar angle from the FOV center and 2π being the full rotational angle. Measurements are made at sets of angles θ_i, with the subscripts 1 and 2 in (2.5) being the breakpoints between adjacent angle points.

The response area at θ_i is obtained from measured channel count rates and monitor detector count rates. For the MAGPD proton calibration at the GSFC accelerators, only one monitor detector is used, and it is mechanically inserted in front of the MAGPD telescope 1 for beam measurements before and after each angle scan set. For this geometry the detection area is calculated from

$$A(E,\Omega_i) = (Ct_{Pi} / T_{Pi}) \times (T_M \times A_M / Ct_M) \qquad (2.6)$$

where

Ct_{Pi} = the 1MP1 through 1MP5 channel counts

T_{Pi} = the counting time for the 1MP1 through 1MP5 counts (s)

Ct_M = monitor counts

T_M = monitor count time (s)

A_M = area of monitor detector = 0.50 cm^2

For the MAGPD electron calibration at the MIT VdeG, two monitor detectors are used in a broad electron beam, and the detection area is calculated from

$$A(E,\Omega_i) = (Ct_{Pi} / T_{Pi}) \times (T_M \times A_{Mj} \times (D_T / D_{Mj})^2) / (Ct_{Mj} \times K_{Mj}) \qquad (2.7)$$

where

Ct_{Pi} = the 1MP1 through 1MP5 channel counts

T_{Pi} = the counting time for the 1MP1 through 1MP5 counts (s)

Ct_{Mj} = M1 (or M2) monitor counts

T_M = Monitor count time (s)

A_{Mj} = area of M1 (or M2) monitor (cm^2)

D_T = distance of telescope 1 detector collimator from electron vacuum exit (in)

D_{Mj} = distance of M1 (or M2) monitor detector from electron vacuum exit (in)

K_{Mj} = normalization factor for M1 (or M2) monitor detector to beam center intensity

The values of the last factor are given by

$$K_{M1} = (M2_{\text{in beam}} / M1_{\text{M2 in beam}}) \times (A_{M1} / A_{M2}) \qquad (2.8)$$

and

$$K_{M2} = (M2_{\text{in beam}} / M1_{M2\text{ in beam}}) \times (M1_{M2\text{ out of beam}} / M2_{\text{out of beam}}) \quad (2.9)$$

The values of (2.8) and (2.9) are generally measured before and after each angle scan set, and the average is used in (2.7).

The MAGPD proton calibration at the GSFC accelerators used measurement sets in θ_i from 0 deg to 15 deg in 5 deg steps, although most sets used θ_i varying from –15 deg to +15 deg in 5 deg steps. Several scans were made to larger angles, to verify the cut-off at 15 deg. The GSFC measurements are made in vacuum, so the only correction to the measured proton energy is for energy loss in the 40 ug/cm^2 Au coating and the 0.5 um Si dead layer on the monitor detector.

The MAGPD electron calibration at the MIT VdeG used measurement sets in θ_i from -40 deg to 40 deg in 10 deg steps, with scans being made in two perpendicular directions labeled "Horizontal" and "Vertical". The two scan directions are used to provide measurement data on the asymmetry of the electron response caused by the electron shielding magnet set in front of the MAGPD telescope SSDs (see Figure 2-1). The electron shielding magnetic field orientations for the nine (9) MAGPD telescopes is shown in Figure 2-2. The electron data were taken with the telescope 1 magnetic field horizontal, and with the magnetic field vertical. The scans were for both positive and negative angles because of the asymmetrical bending of the electron beam, especially for the vertical magnetic field orientation. The resulting integration to get the total MAGPD proton channel geometric factors for electrons uses ¼ of the solid angle factor in (2.5), and sums the four angles for positive and negative θ_i to get the full geometric factor. Note that the 0 degree measurement uses ½ of the solid angle factor in (2.5), since there is only one 0 degree measurement used for each scan.

The sum of (2.4) used the solid angle factors listed in Table 2-1 to calculate the total G(E) for the data taken at GSFC, with the positive and negative angle responses being averaged where both data were available.

Table 2-1. Solid Angle Factor ($\Delta\Omega_i$) Values for GSFC Proton Calibration

θ_i (degrees)	θ_2 / θ_1 (degrees)	$\Delta\Omega_i$ (sr)
0	2.5 / 0	0.005980
5	7.5 / 2.5	0.04777
10	12.5 / 7.5	0.09518
15	17.5 / 12.5	0.14187
20	22.5 / 17.5	0.18747
25	27.5 / 22.55	0.23165
30	32.5 / 27.5	0.27407

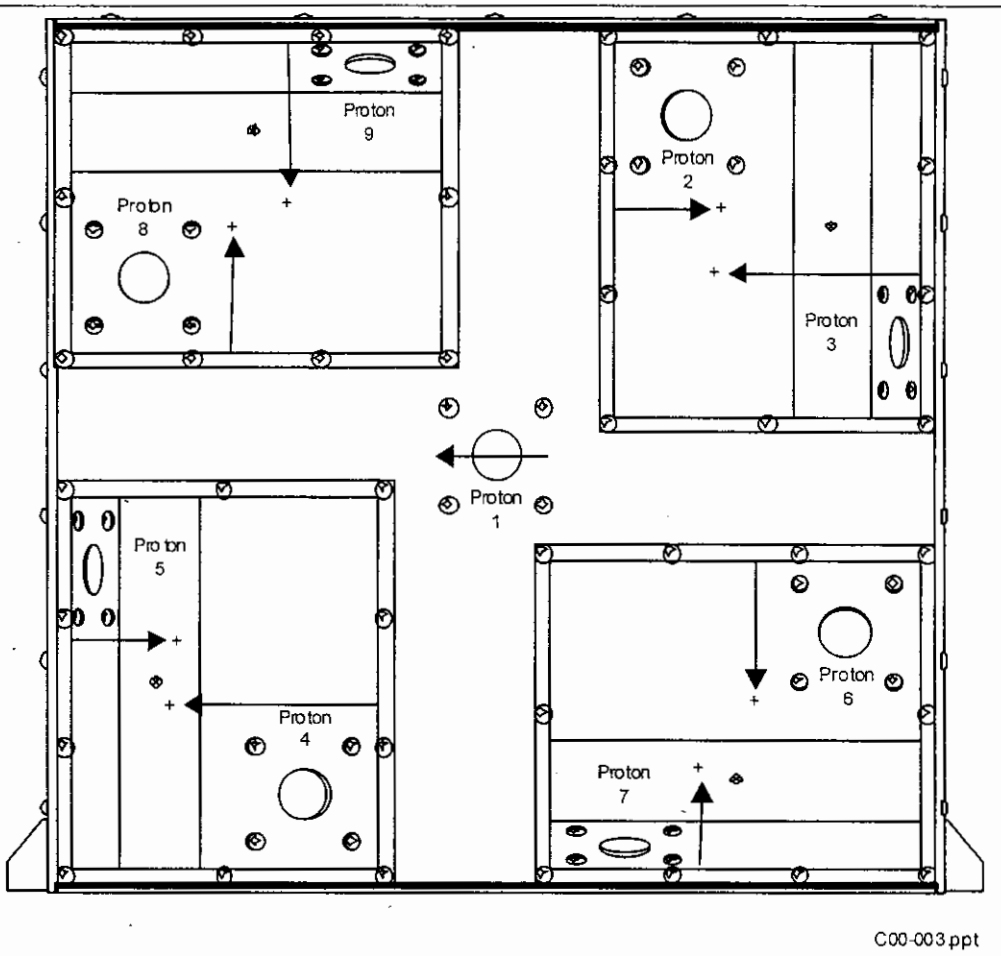

Figure 2-2. Electron Shielding Magnetic Field Orientation in the MAGPD Telescopes

The sum of (2.4) used the solid angle factors listed in Table 2-2 to calculate the total G(E) for the data taken at MIT, with the positive and negative angle responses for both Horizontal and Vertical magnetic field orientations being summed. Note that the 0 degree measurement uses ½ of the solid angle factor in (2.5), since there is only one 0 degree measurement used for each scan, and hence the "2 x" factor in Table 2-2 is used.

Table 2-2. Solid Angle Factor ($\Delta\Omega_i$) Values for MIT Electron Calibration

θ_i (degrees)	θ_2 / θ_1 (degrees)	$\Delta\Omega_i$ (sr)
0	5 / 0	2 x 0.005977
+/-10	15 / 5	0.04755
+/-20	25 / 15	0.09365
+/-30	35 / 25	0.13690
+/-40	45 / 35	0.17600

2.3 Equipment Setup

The basic calibration set-up at the MIT VdeG is shown in Figure 2-3, where the monitor detectors and MAGPD locations are shown. The M2 monitor detector is scanned in front of the MAGPD to provide corrections for a non-uniform electron beam, using the M1 monitor as a reference. During the MAGPD measurements both monitor detectors are used to provide a measure of the electron beam intensity. The air paths to the monitor detectors and to the MAGPD are used to correct the electron beam energy for energy loss in the air. The distances to the monitor detector collimators are used to provide electron beam intensity corrections for the beam at the MAGPD.

The electronics configuration is shown in Figure 2-4, with a portion of the electronics being located in the electron beam room, and some of the electronics being located in the VdeG control room. The monitor detectors were calibrated with the Compton edge of a Cs-137 gamma ray source (477 keV), and this was used along with the full energy peak measured by the monitor detectors to calculate the actual electron beam energy. The VdeG exit window was 0.003 inch of aluminum, and this along with the air paths to the monitor detectors was used to calculate a true VdeG beam energy at the exit window. The air path to the telescope 1 detector was then used to calculate an effective electron energy at the detector, which is the energy for the calibration data. The electron beam energy was thus directly calibrated for each energy data set.

The rotating table in Figure 2-3 was used to perform the azimuth angle scans. For most of the energy measurements the azimuth angle scans were -40 degrees to +40 degrees in 10 degree steps. Each azimuth scan had the 0 degree azimuth point repeated at the end of the scan to verify measurement stability. For data analysis, the multiple 0 degree azimuth points were averaged for the final area value.

The values for some of the constants in (2.7) for the MAGPD electron calibrations at MIT are given below:

T_{1MP1} = the counting time for the 1MP1 channel counts = 16.384 s

T_{1MP2} = the counting time for the 1MP2 channel counts = 16.384 s

T_{1MP3} = the counting time for the 1MP3 channel counts = 16.384 s

T_{1MP4} = the counting time for the 1MP4 channel counts = 32.768 s

T_{1MP5} = the counting time for the 1MP5 channel counts = 32.768 s

T_M = Monitor count time = 10 s

A_{M1} = area of M1 monitor collimator = 0.1734 cm^2

A_{M2} = area of M2 monitor collimator = 0.2027 cm^2

D_{M1} = distance of M1 monitor detector collimator entrance from electron vacuum exit = 25.0 in

D_{M2} = distance of M2 monitor detector collimator entrance from electron vacuum exit = 23.0 in

D_D = distance of the MAGED telescope 1 detector from electron vacuum exit = 30.25 in

The remaining numbers vary for each individual measurement, although the K_{Mj} values are constant for a given electron energy run. The values of K_{Mj} were measured before and after the angle scans at each energy, and the average values are used for the data analysis. Data were checked for reasonable consistency, to ensure that there are no significant variations in electron beam

properties during a particular measurement set. The monitor detectors and 1MPi channel count rates were monitored during the measurements, and the VdeG beam intensity was adjusted to keep the count rates below a level where dead-time effects become important. The VdeG beam occasionally exhibited dark-current pulsations, mostly at the highest energies, and the VdeG had to be "conditioned" at a higher voltage to clean up the beam. Data from such periods was retaken, as necessary, to avoid using data contaminated by high intensity electron/bremsstrahlung background counts.

The electron energy calculations from the monitor detector full energy measurements used the total air path from the VdeG exit window to the detector face, and also included the loss in the 0.3 mil aluminum light shield in front of the monitor detectors. The corrected electron energy at the telescope 1 detector, as calculated from the M1 and M2 monitor detector measurements separately, generally agreed to better than 2%. Electron energy losses in aluminum and air were calculated using the electron stopping powers in Reference 4.

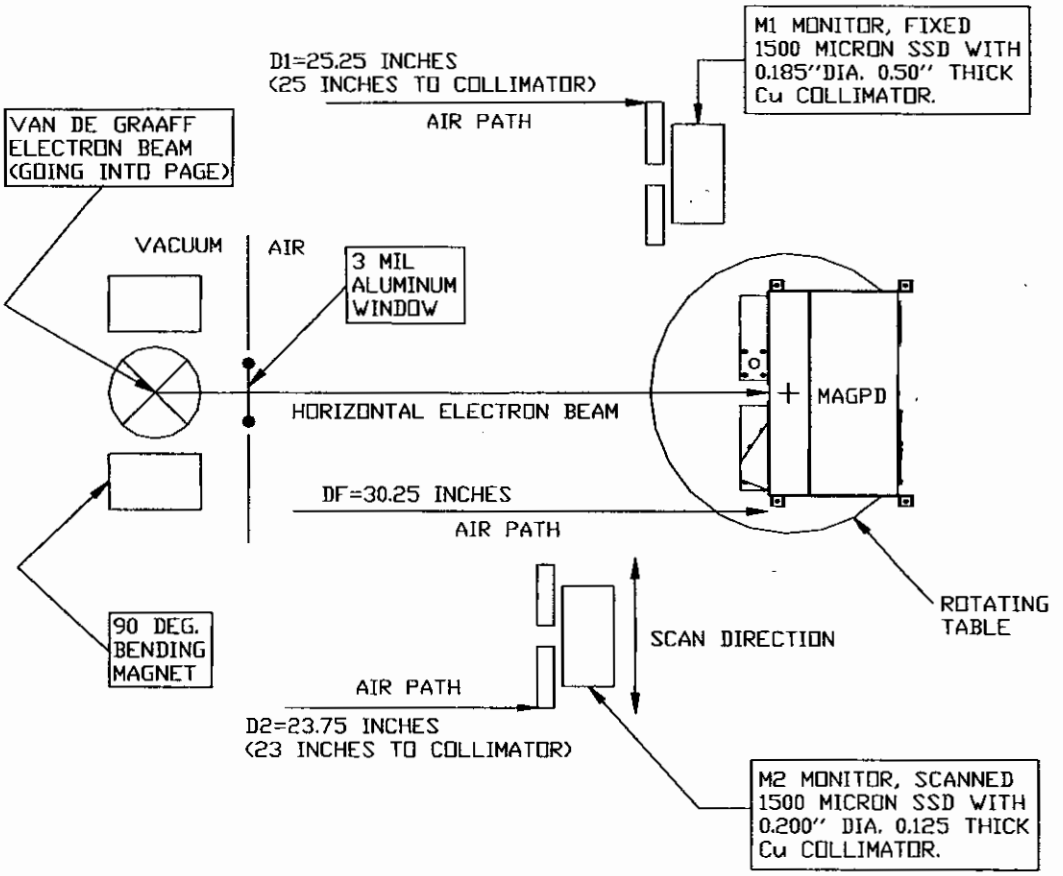

Figure 2-3. Calibration Configuration at MIT Van de Graaff

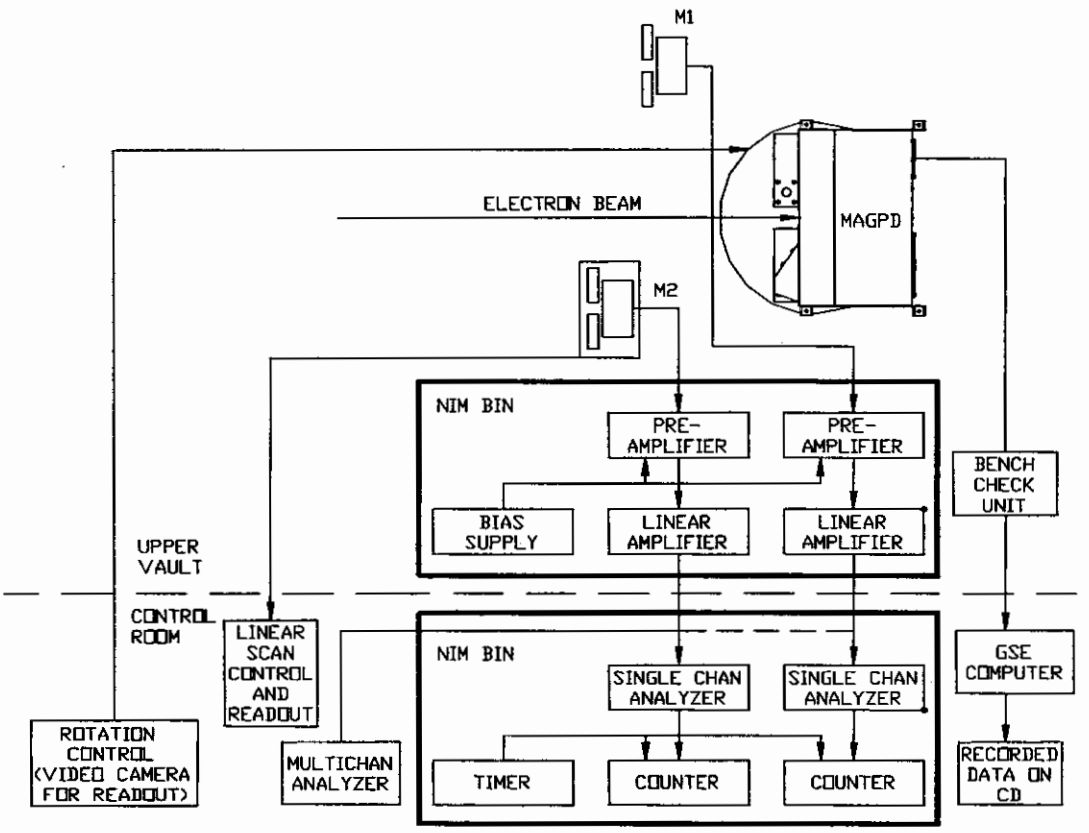

Figure 2-4. Electronics Configuration at MIT Van de Graaff

The basic calibration set-up at the GSFC accelerators is similar to that shown in Figure 2-3 for MIT, except that only one monitor detector is used, and the MAGPD and monitor detector are mounted inside a vacuum chamber. The monitor detector is inserted in front of the MAGPD before and after each angular scan set to provide beam intensity data. Since the measurements are made in vacuum, the only energy loss corrections to the monitor detector measurements is for energy losses in the 40 ug/cm^2 Au layer and the 0.5 um Si dead layer on the monitor detector front surface. The monitor detector is after the beam collimators, and thus the monitor detector detection area is the full area of the monitor detector, or 50 mm^2.

The electronics configuration is also similar to that shown in Figure 2-4 for MIT, again with only one monitor detector being used. For the low energy calibrations, all equipment was located near the Cockroft-Walton accelerator. For the high energy measurements a portion of the electronics is located in the particle beam room, and some of the electronics is located in the VdeG control room. The monitor detector was calibrated either with the 59.54 keV x-ray from Am-241 (low energy accelerator measurements), or with the 5.48 MeV alpha particle from Am-241 (high energy accelerator measurements). The monitor detector

beam energy measurements were corrected to provide a true beam energy. The particle beam energy was thus directly calibrated for each energy data set.

For the GSFC calibrations, the rotating table in Figure 2-3 was replaced by a rotating vacuum feedthru shaft, which was used to perform the azimuth angle scans. For most of the energy measurements the azimuth angle scans were -15 degrees to +15 degrees in 5 degree steps. Each azimuth scan had the 0 degree azimuth point repeated at the end of the scan to verify measurement stability. For data analysis, the multiple 0 degree azimuth points were averaged for the final area value.

The values for some of the constants in (2.6) for the MAGPD calibrations at GSFC are given below.

T_{1MP1} = the counting time for the 1MP1 channel counts = 16.384 s

T_{1MP2} = the counting time for the 1MP2 channel counts = 16.384 s

T_{1MP3} = the counting time for the 1MP3 channel counts = 16.384 s

T_{1MP4} = the counting time for the 1MP4 channel counts = 32.768 s

T_{1MP5} = the counting time for the 1MP5 channel counts = 32.768 s

T_M = Monitor count time = 1 s

A_M = area of monitor detector = 0.500 cm^2

The remaining numbers vary for each individual measurement. Data were checked for reasonable consistency, to ensure that there were no significant variations in electron beam properties during a particular measurement set. The monitor detector and 1MPi channel count rates were monitored during the measurements, and the accelerator beam intensity was adjusted to keep the count rates below a level where dead-time effects become important.

The particle energy calculations from the monitor detector measurements used the electron energy losses in Au and Si from Refs. 4 and 5, while the proton data came from Ref. 6.

3.0 DATA ANALYSIS AND RESULTS

3.1 Measured Detector Areas

3.1.1 1MPi Proton Channel Measured Areas for Protons at GSFC

The telescope 1 measured 1MPi channel areas for protons at GSFC for several energies are summarized in Tables 3-1 to 3-16. The calibrated proton energy measured by the GSFC monitor detector is listed for each measurement. The areas are calculated from the monitor detector area, using the procedure described in Section 2.2. Measurements for most proton energies covered the range of -15 deg to +15 deg in 5 deg steps in azimuth, with a few energies having only 0 degree measurements. A few energies had slightly larger angle sets measured to verify the sharp cut-off at +/-15 deg. The last Table 3-16 has the results for the 0 degree area measurements for several energies that have no angular scan, but were made to provide better channel energy edge resolution.

Plots of the measured areas are shown in Figure 3-1 for 1MP2 and 1MP3 at 111.3 keV, which is at the transition of the response for the two channels, and in Figure 3-2 for 1MP1, 1MP2 and 1MP3 at 122.5 keV, which is well within the 1MP2 response band. Since the measurements are made in vacuum with a very narrow angular spread to the proton beam, the data show the cut-off at +/-15 deg, in agreement with the calculated response.

Table 3-1. Measured 1MPi Detection Areas in cm^2 for 69.1 keV Protons

Angle (°)	Area (cm^2)				
	1MP1	1MP2	1MP3	1MP4	1MP5
0	3.27E-05	0	0	0	0
5	1.11E-05	0	0	0	0
10	0	0	0	0	0

Table 3-2. Measured 1MPi Detection Areas in cm^2 for 74.2 keV Protons

Angle (°)	Area (cm^2)				
	1MP1	1MP2	1MP3	1MP4	1MP5
0	1.36E-03	0	0	0	0
5	1.38E-03	0	0	0	0
10	1.78E-04	0	0	0	0
15	0	0	0	0	0
0	1.31E-03	0	0	0	0
-5	8.99E-04	0	0	0	0
-10	2.07E-04	1.09E-05	0	0	0

Table 3-3. Measured 1MPi Detection Areas in cm^2 for 79.3 keV Protons

Angle (°)	Area (cm^2)				
	1MP1	1MP2	1MP3	1MP4	1MP5
0	1.63E-02	0	0	0	0
5	1.53E-02	0	0	0	0
10	5.19E-03	0	0	0	0
15	0	0	0	0	0
0	1.74E-02	0	0	0	0
-5	1.29E-02	0	0	0	0
-10	2.11E-03	9.89E-06	0	0	0

Table 3-4. Measured 1MPi Detection Areas in cm^2 for 85.0 keV Protons

Angle (°)	Area (cm^2)				
	1MP1	1MP2	1MP3	1MP4	1MP5
0	5.49E-02	0	0	0	0
5	5.42E-02	9.85E-06	0	0	0
10	2.26E-02	0	0	0	0
15	1.88E-05	0	0	0	0
0	5.49E-02	0	0	0	0
-5	4.67E-02	0	0	0	0
-10	1.11E-02	0	0	0	0

Table 3-5. Measured 1MPi Detection Areas in cm^2 for 97.8 keV Protons

Angle (°)	Area (cm^2)				
	1MP1	1MP2	1MP3	1MP4	1MP5
0	6.75E-02	0	0	0	0
5	6.84E-02	7.63E-06	0	0	0
10	4.00E-02	7.63E-06	0	0	0
15	4.47E-05	0	0	0	0
20	0	0	0	0	0
0	6.67E-02	7.44E-06	0	0	0
-5	5.74E-02	2.26E-05	0	0	0
-10	1.27E-02	7.44E-06	0	0	0

Table 3-6. Measured 1MPi Detection Areas in cm^2 for 106.9 keV Protons

Angle (°)	Area (cm^2)				
	1MP1	1MP2	1MP3	1MP4	1MP5
0	5.37E-02	2.86E-03	0	0	0
5	5.05E-02	2.28E-03	0	0	0
10	2.13E-02	6.04E-04	0	0	0
15	0	0	0	0	0
0	5.49E-02	3.09E-03	0	0	0
-5	5.28E-02	2.27E-03	0	0	0
-10	1.91E-02	3.19E-04	0	0	0
-15	0	0	0	0	0

Table 3-7. Measured 1MPi Detection Areas in cm^2 for 111.3 keV Protons

Angle (°)	Area (cm^2)				
	1MP1	1MP2	1MP3	1MP4	1MP5
0	4.60E-02	2.69E-02	0	0	0
5	4.49E-02	2.77E-02	0	0	0
10	3.07E-02	1.17E-02	0	0	0
15	3.32E-05	6.63E-06	0	0	0
0	4.21E-02	2.62E-02	0	0	0
-5	4.46E-02	2.13E-02	0	0	0
-10	1.06E-02	3.52E-03	0	0	0

Table 3-8. Measured 1MPi Detection Areas in cm^2 for 116.7 keV Protons

Angle (°)	Area (cm^2)				
	1MP1	1MP2	1MP3	1MP4	1MP5
0	6.36E-03	6.67E-02	0	0	0
5	6.29E-03	6.59E-02	0	0	0
10	4.64E-03	3.52E-02	0	0	0
15	7.54E-06	2.26E-05	0	0	0
0	5.09E-03	6.48E-02	0	0	0
-5	5.93E-03	5.54E-02	0	0	0
-10	2.67E-03	1.31E-02	0	0	0
-15	0	0	0	0	0

Table 3-9. Measured 1MPi Detection Areas in cm^2 for 122.5 keV Protons

Angle (°)	Area (cm^2)				
	1MP1	1MP2	1MP3	1MP4	1MP5
0	4.35E-04	6.80E-02	5.65E-06	0	0
5	4.85E-04	6.86E-02	5.70E-06	0	0
10	4.43E-04	3.61E-02	0	0	0
15	1.19E-05	1.78E-05	0	0	0
0	5.55E-04	7.56E-02	0	0	0
-5	4.90E-04	6.36E-02	0	0	0
-10	2.92E-04	1.73E-02	0	0	0
-15	0	0	0	0	0

Table 3-10. Measured 1MPi Detection Areas in cm^2 for 157 keV Protons

Angle (°)	Area (cm^2)				
	1MP1	1MP2	1MP3	1MP4	1MP5
0	1.40E-04	1.92E-01	2.39E-04	1.40E-05	0
5	1.55E-04	1.83E-01	2.25E-04	0	0
10	6.94E-05	6.57E-02	0	1.39E-05	0
15	0	0	0	0	0
0	2.36E-04	2.01E-01	2.08E-04	6.94E-06	0
-5	1.82E-04	1.92E-01	2.39E-04	7.02E-06	0
-10	2.81E-05	1.12E-01	2.81E-05	7.02E-06	0
-15	1.42E-05	0	0	0	0

Table 3-11. Measured 1MPi Detection Areas in cm^2 for 200 keV Protons

Angle (°)	Area (cm^2)				
	1MP1	1MP2	1MP3	1MP4	1MP5
0	7.40E-05	2.77E-04	1.85E-01	8.32E-05	4.62E-06
5	2.77E-05	1.85E-04	1.75E-01	2.31E-05	1.39E-05
10	2.80E-05	8.39E-05	7.10E-02	9.32E-06	0
15	9.54E-06	9.54E-06	0	0	0
0	9.32E-05	3.35E-04	1.86E-01	4.19E-05	4.66E-06
-5	5.59E-05	2.05E-04	1.67E-01	9.32E-06	0
-10	2.77E-05	1.39E-04	1.21E-01	4.62E-06	0
-15	9.25E-06	1.85E-05	2.77E-05	0	0

Table 3-12. Measured 1MPi Detection Areas in cm^2 for 218 keV Protons

Angle (°)	Area (cm^2)				
	1MP1	1MP2	1MP3	1MP4	1MP5
0	6.43E-05	2.17E-04	9.26E-02	2.81E-05	0
5	1.58E-04	2.85E-04	9.32E-02	1.48E-05	9.84E-06
10	0	4.50E-05	2.13E-02	0	0
15	0	8.25E-06	0	0	0
0	1.13E-04	1.83E-04	6.31E-02	8.73E-06	0
-5	1.75E-05	1.13E-04	4.89E-02	4.36E-06	0
-10	3.39E-05	9.33E-05	3.07E-02	0	0
-15	0	2.54E-05	2.54E-05	0	0
0	1.31E-04	1.66E-04	6.68E-02	4.37E-06	0

Table 3-13. Measured 1MPi Detection Areas in cm^2 for 241 keV Protons

Angle (°)	Area (cm^2)				
	1MP1	1MP2	1MP3	1MP4	1MP5
0	8.14E-05	6.78E-05	1.08E-01	4.44E-03	6.78E-06
5	8.32E-05	2.77E-05	7.63E-02	5.93E-03	6.94E-06
10	4.16E-05	2.77E-05	3.82E-02	1.82E-03	0
15	0	0	0	0	0
0	1.04E-04	2.23E-04	1.19E-01	6.36E-03	0
-5	8.83E-05	1.18E-04	1.28E-01	7.67E-03	2.94E-05
-10	2.91E-05	8.72E-05	1.11E-01	4.53E-03	7.27E-06
-15	0	2.84E-05	3.98E-04	7.10E-06	0

Table 3-14. Measured 1MPi Detection Areas in cm^2 for 274 keV Protons

Angle (°)	Area (cm^2)				
	1MP1	1MP2	1MP3	1MP4	1MP5
0	5.55E-05	1.11E-04	2.50E-04	8.34E-02	0
5	5.55E-05	1.53E-04	3.05E-04	8.34E-02	2.08E-05
10	1.36E-05	0	2.71E-05	3.39E-02	0
15	0	0	0	0	0
0	5.75E-05	1.44E-04	1.87E-04	7.90E-02	7.18E-06
-5	1.15E-04	2.87E-05	1.87E-04	6.80E-02	7.18E-06
-10	1.40E-05	5.61E-05	2.81E-05	3.68E-02	7.02E-06
-15	0	0	2.91E-04	1.39E-05	0

Table 3-15. Measured 1MPi Detection Areas in cm^2 for 521 keV Protons

Angle (°)	Area (cm^2)				
	1MP1	1MP2	1MP3	1MP4	1MP5
0	2.46E-04	4.55E-04	2.92E-04	2.82E-04	1.54E-01
5	1.32E-04	3.51E-04	2.11E-04	1.49E-04	1.20E-01
10	2.69E-05	1.88E-04	5.39E-05	6.28E-05	3.25E-02
15	0	0	0	0	4.07E-06
0	2.82E-04	5.38E-04	2.46E-04	2.69E-04	1.10E-01
-5	2.33E-04	5.34E-04	3.79E-04	3.83E-04	9.92E-02
-10	3.30E-05	1.40E-04	8.25E-05	4.54E-05	2.59E-02
-15	0	0	0	0	0

Table 3-16. Additional Measured 1MPi 0 Degree Detection Areas in cm^2 for Protons

Proton Energy (keV)	Area (0 degrees) (cm^2)				
	1MP1	1MP2	1MP3	1MP4	1MP5
167	3.39E-05	7.91E-03	1.26E-02	5.65E-06	0
177	1.02E-04	1.27E-03	2.26E-01	3.96E-05	0
188	4.21E-05	3.37E-04	1.60E-01	1.58E-05	0
253	7.63E-05	6.10E-05	2.12E-03	3.64E-02	7.63E-06
264	4.36E-05	1.16E-04	1.31E-04	5.25E-02	0
315	6.49E-05	7.79E-05	3.90E-05	6.17E-03	0
347	1.39E-05	5.55E-05	9.72E-05	1.55E-02	2.64E-02
358	1.43E-04	2.34E-04	1.04E-04	5.26E-04	6.15E-02
419	2.47E-04	2.60E-05	1.30E-05	0	1.62E-04
672	7.18E-05	2.99E-04	1.20E-04	1.02E-04	3.29E-02
775	7.18E-05	1.98E-04	3.82E-04	1.26E-04	1.79E-01
785	9.42E-05	1.47E-04	2.99E-04	1.15E-04	2.14E-01
792	1.82E-05	2.73E-05	1.37E-04	3.19E-05	5.97E-04
797	1.62E-05	1.62E-05	1.38E-04	2.84E-05	5.63E-04
808	1.03E-05	9.27E-05	3.19E-04	7.73E-05	1.67E-04

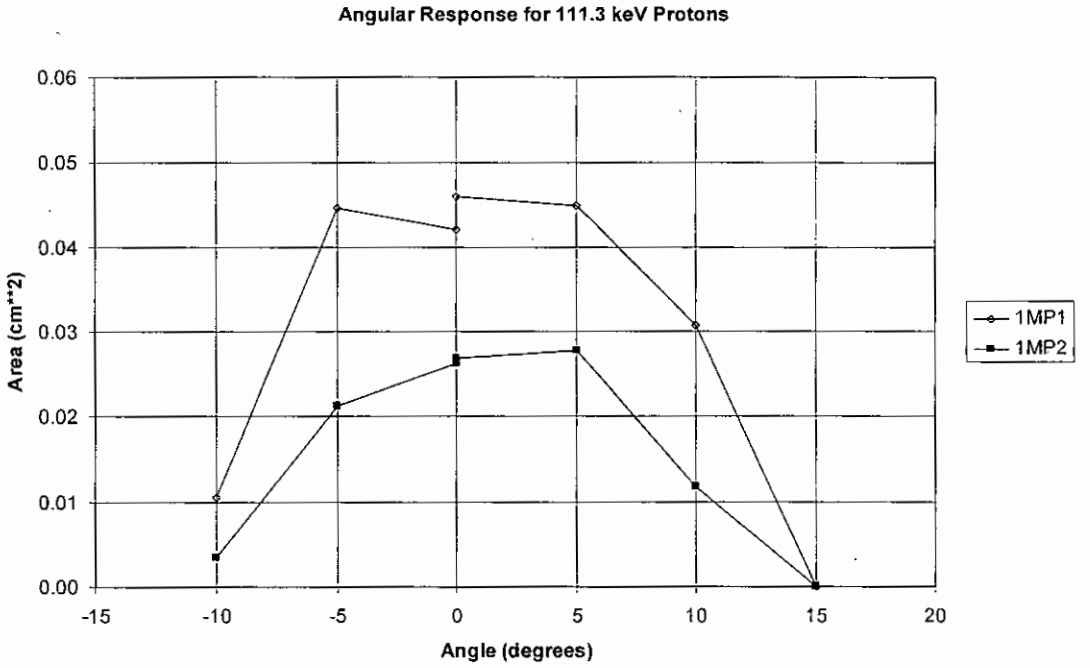

Figure 3-1. Angular Response of 1MP1 and 1MP2 at 111.3 keV

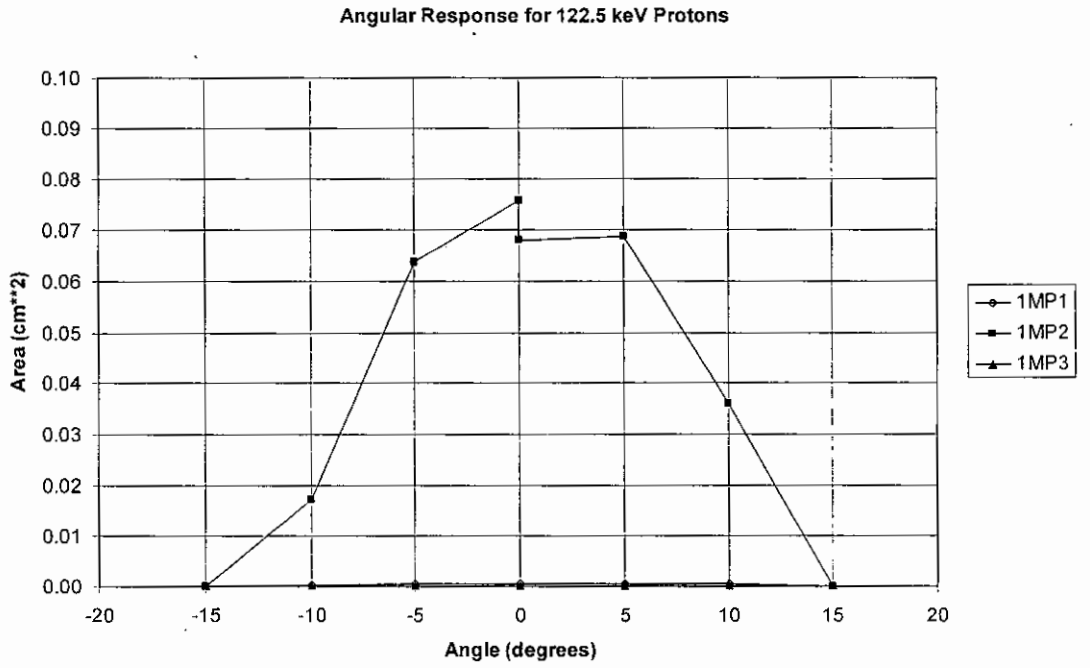

Figure 3-2. Angular Response of 1MP1, 1MP2 and 1MP3 at 122.5 keV

3.1.2 1MPi Proton Channel Measured Areas for Electrons at MIT

The telescope 1 measured 1MPi channel areas for electrons at several energies are summarized in Tables 3-17 to 3-28. The calibrated electron energy at the telescope 1 detector is listed for each measurement. The areas are calculated from the two monitor detector collimator areas, using the procedure described in Section 2.2. Measurements for all electron energies covered the range of -40 deg to +40 deg in 10 deg steps in azimuth.

Angular plots of the measured areas for 770 keV electrons are shown in Figure 3-3 for the Vertical scan, and in Figure 3-4 for the Horizontal scan, for 1MP1, 1MP2 and 1MP3. The Vertical scan measurements have the magnetic field pointing up, so the measured angular distribution is skewed towards negative angles because of the bending of the electrons. Measurements at the MIT VdeG are made in air, with the electron beam exiting vacuum through a 3 mil Al foil, so there is significant scattering of the electron beam, which broadens the beam angular distribution.

Table 3-17. Measured 1MPi Detection Areas in cm^2 for 770 keV Electrons (Horizontal)

Angle (°)	Area (cm^2)				
	1MP1	1MP2	1MP3	1MP4	1MP5
0	1.19E-04	3.98E-04	2.65E-04	3.45E-04	1.19E-04
-40	1.57E-05	7.87E-05	3.15E-05	7.87E-05	6.29E-05
-30	5.41E-05	1.08E-04	1.80E-05	1.62E-04	0
-20	0	7.69E-05	1.54E-04	2.05E-04	7.69E-05
-10	1.27E-04	2.73E-04	1.45E-04	1.09E-04	2.00E-04
0	1.19E-04	2.88E-04	2.71E-04	2.71E-04	1.36E-04
10	1.58E-04	4.29E-04	1.58E-04	2.26E-04	6.78E-05
20	8.66E-05	1.95E-04	8.66E-05	1.08E-04	1.08E-04
30	4.20E-05	1.54E-04	5.61E-05	9.81E-05	4.20E-05
40	1.52E-05	0	0	3.03E-05	0

Table 3-18. Measured 1MPi Detection Areas in cm^2 for 802 keV Electrons (Horizontal)

Angle (°)	Area (cm^2)				
	1MP1	1MP2	1MP3	1MP4	1MP5
0	2.12E-04	5.05E-04	2.93E-04	2.77E-04	1.30E-04
-40	0	6.74E-05	4.04E-05	1.08E-04	5.39E-05
-30	6.19E-05	1.08E-04	4.64E-05	3.10E-05	1.55E-05
-20	0	2.55E-04	1.18E-04	1.96E-04	5.88E-05
-10	2.07E-04	3.10E-04	2.07E-04	2.48E-04	1.65E-04
0	1.97E-04	5.20E-04	2.15E-04	3.23E-04	1.97E-04
10	1.65E-04	5.35E-04	1.53E-04	2.55E-04	1.65E-04
20	3.90E-05	2.21E-04	1.56E-04	6.51E-05	1.17E-04
30	1.03E-04	1.55E-04	2.58E-05	7.74E-05	6.45E-05
40	2.62E-05	6.55E-05	0	3.93E-05	0
0	9.06E-05	4.89E-04	1.63E-04	1.45E-04	1.63E-04

Table 3-19. Measured 1MPi Detection Areas in cm^2 for 1140 keV Electrons (Horizontal)

Angle (°)	Area (cm^2)				
	1MP1	1MP2	1MP3	1MP4	1MP5
0	2.20E-04	9.27E-04	2.29E-04	2.10E-04	1.72E-04
-40	0	1.30E-04	1.30E-05	2.60E-05	1.30E-05
-30	4.95E-05	1.88E-04	4.95E-05	8.92E-05	9.91E-06
-20	1.38E-04	5.23E-04	5.92E-05	1.78E-04	5.92E-05
-10	2.42E-04	8.15E-04	1.70E-04	1.86E-04	1.61E-04
0	2.34E-04	1.01E-03	2.18E-04	3.89E-04	1.56E-04
10	3.05E-04	7.85E-04	2.40E-04	2.40E-04	1.74E-04
20	1.29E-04	5.44E-04	1.29E-04	2.58E-04	5.73E-05
30	4.53E-05	1.51E-04	7.55E-05	1.21E-04	4.53E-05
40	0	5.26E-05	1.31E-05	2.63E-05	1.31E-05
0	2.34E-04	7.84E-04	2.24E-04	2.75E-04	1.73E-04

Table 3-20. Measured 1MPi Detection Areas in cm^2 for 1620 keV Electrons (Horizontal)

Angle (°)	Area (cm^2)				
	1MP1	1MP2	1MP3	1MP4	1MP5
0	5.49E-04	1.15E-03	2.70E-04	4.28E-04	1.40E-04
-40	3.24E-05	5.39E-05	0	0	0
-30	7.47E-05	2.24E-04	8.96E-05	5.97E-05	0
-20	3.95E-04	8.42E-04	1.45E-04	1.04E-04	4.16E-05
-10	4.80E-04	1.20E-03	3.51E-04	3.14E-04	9.23E-05
0	7.03E-04	1.48E-03	3.58E-04	2.65E-04	7.95E-05
10	5.64E-04	1.32E-03	2.56E-04	2.56E-04	1.49E-04
20	2.11E-04	5.49E-04	2.03E-04	1.10E-04	6.75E-05
30	1.62E-04	2.20E-04	4.63E-05	6.95E-05	3.48E-05
40	1.47E-05	1.18E-04	2.94E-05	1.47E-05	2.94E-05
0	8.33E-04	1.43E-03	2.82E-04	2.54E-04	1.13E-04

Table 3-21. Measured 1MPi Detection Areas in cm^2 for 2100 keV Electrons (Horizontal)

Angle (°)	Area (cm^2)				
	1MP1	1MP2	1MP3	1MP4	1MP5
0	1.35E-03	1.80E-03	4.50E-04	2.25E-04	2.70E-04
-40	0	1.55E-04	3.89E-05	3.89E-05	0
-30	1.43E-04	4.46E-04	3.71E-05	0	7.43E-05
-20	3.61E-04	1.05E-03	1.61E-04	1.61E-04	8.05E-05
-10	1.54E-03	1.92E-03	2.31E-04	3.84E-04	2.31E-04
0	1.79E-03	2.30E-03	5.34E-04	3.28E-04	2.05E-04
10	1.23E-03	1.49E-03	3.90E-04	2.13E-04	1.77E-04
20	8.09E-04	8.14E-04	1.11E-04	2.59E-04	1.48E-04
30	3.33E-04	2.87E-04	2.87E-05	5.74E-05	2.87E-05
40	5.47E-05	2.34E-04	8.49E-05	4.25E-05	0
0	8.04E-07	2.79E-03	5.62E-04	4.01E-04	1.61E-04

Table 3-22. Measured 1MPi Detection Areas in cm^2 for 2600 keV Electrons (Horizontal)

Angle (°)	Area (cm^2)				
	1MP1	1MP2	1MP3	1MP4	1MP5
0	5.59E-03	5.59E-03	2.17E-03	1.75E-03	6.02E-04
-40	1.01E-03	1.31E-03	8.94E-04	7.74E-04	2.80E-04
-30	1.47E-03	2.26E-03	2.07E-03	9.87E-04	5.94E-04
-20	1.60E-03	2.34E-03	1.05E-03	1.98E-03	4.89E-04
-10	8.82E-03	8.82E-03	3.38E-03	2.30E-03	8.41E-04
0	1.09E-02	8.98E-03	4.00E-03	3.42E-03	1.18E-03
10	2.85E-03	3.74E-03	1.66E-03	1.97E-03	5.41E-04
20	2.10E-03	2.89E-03	1.10E-03	1.80E-03	7.17E-04
30	2.38E-03	2.97E-03	2.03E-03	2.03E-03	8.62E-04
40	1.28E-03	1.54E-03	1.09E-03	1.35E-03	6.34E-04
0	1.15E-02	9.28E-03	4.63E-03	3.96E-03	1.43E-03

Table 3-23. Measured 1MPi Detection Areas in cm^2 for 770 keV Electrons (Vertical)

Angle (°)	Area (cm^2)				
	1MP1	1MP2	1MP3	1MP4	1MP5
0	2.32E-04	8.67E-04	4.80E-04	4.02E-04	2.94E-04
-40	1.56E-05	6.26E-05	3.13E-05	7.82E-05	4.69E-05
-30	1.13E-04	3.01E-04	1.32E-04	1.88E-04	1.88E-04
-20	1.54E-04	8.34E-04	3.95E-04	5.27E-04	2.42E-04
-10	2.04E-04	8.56E-04	3.26E-04	4.48E-04	3.26E-04
0	1.44E-04	9.55E-04	3.24E-04	3.96E-04	4.15E-04
10	2.46E-04	5.67E-04	3.40E-04	3.97E-04	2.08E-04
20	1.06E-04	4.23E-04	1.76E-04	2.47E-04	7.05E-05
30	1.04E-04	1.90E-04	3.46E-05	1.21E-04	1.04E-04
40	0	1.37E-04	1.95E-05	0	1.95E-05
0	3.20E-04	7.08E-04	5.48E-04	5.93E-04	2.97E-04

Table 3-24. Measured 1MPi Detection Areas in cm^2 for 870 keV Electrons (Vertical)

Angle (°)	Area (cm^2)				
	1MP1	1MP2	1MP3	1MP4	1MP5
0	4.20E-04	1.16E-03	3.55E-04	4.84E-04	3.23E-04
-40	4.62E-05	4.62E-05	4.62E-05	0	9.25E-05
-30	1.48E-04	6.93E-04	4.95E-05	4.95E-05	1.48E-04
-20	4.79E-04	1.07E-03	2.66E-04	3.73E-04	2.13E-04
-10	3.73E-04	1.34E-03	3.36E-04	5.60E-04	2.24E-04
0	2.14E-04	1.02E-03	5.36E-04	4.82E-04	1.61E-04
10	5.03E-04	7.77E-04	4.11E-04	2.74E-04	0
20	1.17E-04	7.00E-04	1.17E-04	2.92E-04	1.17E-04
30	1.33E-04	3.98E-04	2.21E-04	1.33E-04	8.85E-05
40	4.35E-05	8.69E-05	4.35E-05	4.35E-05	0
0	1.68E-04	7.27E-04	2.80E-04	6.15E-04	5.59E-05

Table 3-25. Measured 1MPi Detection Areas in cm^2 for 1140 keV Electrons (Vertical)

Angle (°)	Area (cm^2)				
	1MP1	1MP2	1MP3	1MP4	1MP5
0	7.19E-04	1.53E-03	2.88E-04	6.04E-04	2.59E-04
-40	1.03E-04	2.67E-04	6.15E-05	1.03E-04	0
-30	1.08E-03	2.30E-03	2.44E-04	2.71E-04	2.71E-05
-20	1.32E-03	3.04E-03	3.76E-04	2.82E-04	2.51E-04
-10	8.05E-04	1.98E-03	5.47E-04	5.75E-04	4.03E-04
0	4.52E-04	2.10E-03	5.48E-04	5.16E-04	4.19E-04
10	3.24E-04	8.38E-04	1.89E-04	2.16E-04	8.11E-05
20	1.15E-04	2.87E-04	7.19E-05	1.29E-04	4.31E-05
30	1.48E-04	3.15E-04	1.30E-04	7.41E-05	1.30E-04
40	2.93E-05	1.17E-04	2.93E-05	8.80E-05	2.93E-05
0	3.61E-04	1.03E-03	1.55E-04	3.35E-04	1.55E-04

Table 3-26. Measured 1MPi Detection Areas in cm^2 for 1620 keV Electrons (Vertical)

Angle (°)	Area (cm^2)				
	1MP1	1MP2	1MP3	1MP4	1MP5
0	6.92E-04	2.08E-03	3.64E-04	8.38E-04	3.28E-04
-40	5.15E-05	1.54E-04	1.03E-04	0	0
-30	2.75E-03	4.23E-03	5.98E-04	3.99E-04	1.20E-04
-20	7.23E-03	1.38E-02	1.28E-03	6.41E-04	5.25E-04
-10	5.53E-03	9.90E-03	1.77E-03	1.29E-03	5.36E-04
0	3.25E-03	7.23E-03	1.32E-03	1.32E-03	6.05E-04
10	3.99E-04	9.11E-04	2.50E-04	3.24E-04	9.98E-05
20	4.23E-04	1.06E-03	1.90E-04	1.31E-04	7.29E-05
30	0	7.62E-04	0	1.09E-04	0
40	4.93E-04	3.70E-04	0	1.23E-04	0
0	8.72E-04	1.82E-03	4.00E-04	2.91E-04	1.09E-04

Table 3-27. Measured 1MPi Detection Areas in cm^2 for 2100 keV Electrons (Vertical)

Angle (°)	Area (cm^2)				
	1MP1	1MP2	1MP3	1MP4	1MP5
0	1.44E-03	2.61E-03	3.76E-04	2.21E-04	1.33E-04
-40	1.51E-04	3.01E-04	3.76E-05	1.88E-05	1.88E-05
-30	6.96E-04	1.56E-03	2.64E-04	1.44E-04	7.20E-05
-20	2.33E-03	3.74E-03	4.65E-04	4.65E-04	2.13E-04
-10	4.11E-03	9.18E-03	1.41E-03	6.57E-04	2.70E-04
0	1.96E-03	4.62E-03	5.48E-04	1.57E-03	5.87E-04
10	7.93E-04	1.30E-03	2.83E-04	1.13E-04	5.66E-05
20	1.56E-04	3.91E-04	1.56E-04	0	0
30	3.06E-04	5.10E-04	1.02E-04	1.02E-04	0
40	8.57E-05	1.71E-04	8.57E-05	0	0
0	1.98E-03	2.74E-03	5.66E-04	3.78E-04	0

Table 3-28. Measured 1MPi Detection Areas in cm^2 for 2600 keV Electrons (Vertical)

Angle (°)	Area (cm^2)				
	1MP1	1MP2	1MP3	1MP4	1MP5
0	2.14E-02	1.53E-02	6.15E-03	5.12E-03	1.70E-03
-40	2.92E-03	3.82E-03	2.67E-03	2.78E-03	1.06E-03
-30	4.64E-03	5.76E-03	3.02E-03	3.44E-03	1.36E-03
-20	3.87E-03	5.34E-03	3.17E-03	2.90E-03	1.27E-03
-10	2.09E-02	1.52E-02	5.82E-03	5.22E-03	1.90E-03
0	1.72E-02	1.25E-02	4.98E-03	4.75E-03	1.93E-03
10	4.98E-03	5.47E-03	2.97E-03	3.61E-03	1.24E-03
20	4.15E-03	5.69E-03	2.84E-03	3.00E-03	1.03E-03
30	1.77E-03	2.56E-03	1.15E-03	1.33E-03	6.30E-04
40	7.42E-04	7.83E-04	6.31E-04	6.00E-04	2.24E-04
0	8.30E-03	6.91E-03	3.30E-03	3.44E-03	8.10E-04

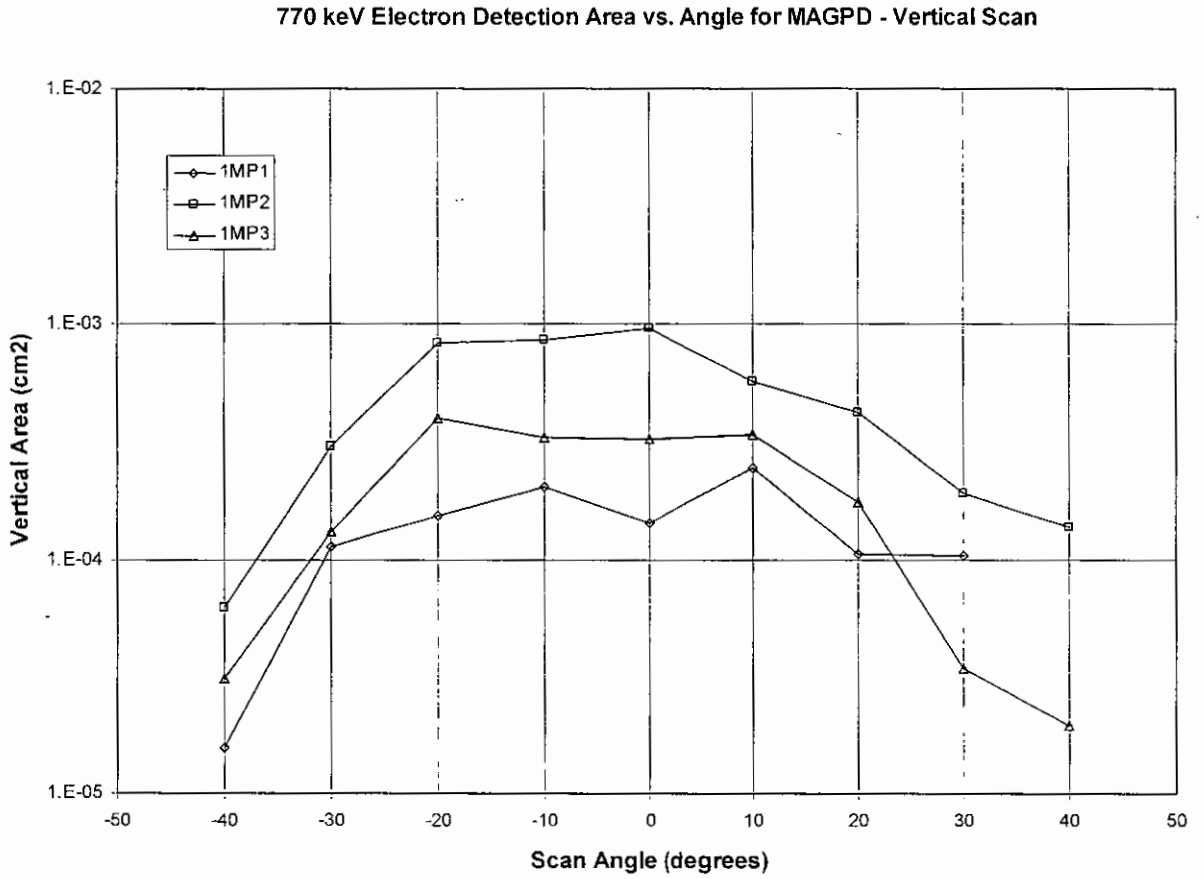

Figure 3-3. Vertical Angular Response of 1MP1, 1MP2 and 1MP3 for 770 keV Electrons

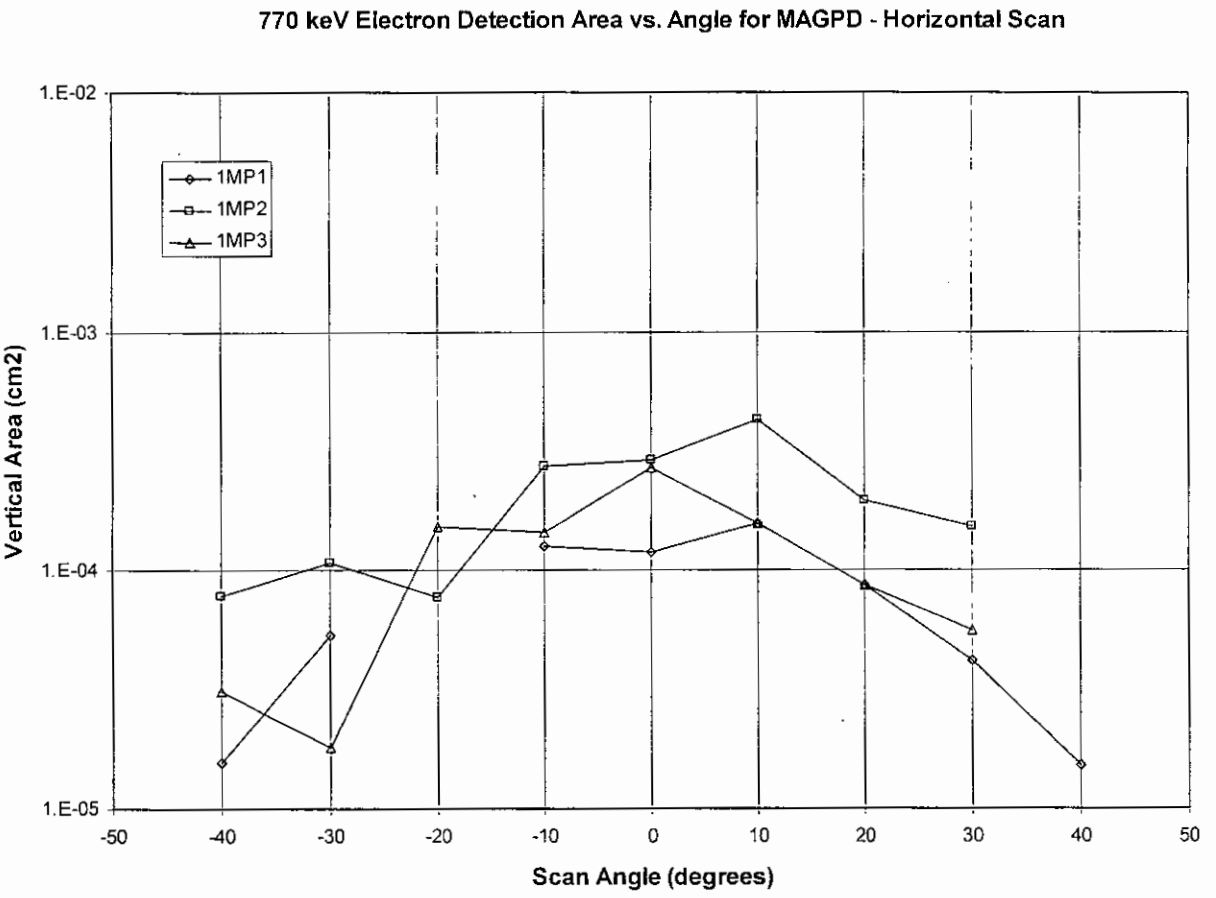

Figure 3-4. Horizontal Angular Response of 1MP1, 1MP2 and 1MP3 for 770 keV Electrons

The MAGPD electron shielding magnets are shown in the telescope design in Figure 2-1, and the direction for the magnetic field in each telescope is shown in Figure 2-2. The Horizontal electron response scans at MIT were measured with the Telescope 1 magnetic field horizontal, mounted as shown in Figure 2-3, with the magnetic field pointing upward in the figure plane. Positive angle rotation of the MAGPD had the Telescope 1 FOV direction rotating upward in the plane of Figure 2-3, while negative angles had the FOV direction rotating down. For the Vertical electron scans the MAGPD was rotated 90 degrees from the Figure 2-3 position, with the Telescope 1 magnetic field pointing up out of the Figure plane. Rotation angles were the same as for the Horizontal scans. Electrons entering the MAGPD telescope are bent by the magnetic field, such that for the Vertical magnetic field scans the electrons will bend upward in the plane of Figure 2-3. This results in the lower energy electron response for the Vertical scans being displaced towards negative rotation angles, as is shown by the 1MP2 plot in Figure 3-3. The Horizontal scans have negligible +/- angle shifts, as shown by the data plotted in Figure 3-4. Protons show negligible bending in the magnetic field, as shown by the data plotted in Figures 3-1 and 3-2.

3.2 Measured Geometric Factors

3.2.1 Proton Geometric Factors

The measured proton geometric factors from Section 3.1.1, obtained by integrating over the GSFC angular measurements given in Tables 3-1 through 3-15, for all 1MPi channels, are summarized in Table 3-29. The average A(0) area values from the GSFC measurements in Tables 3-1 through 3-16 are in Table 3-30. The total geometric factor in Table 3-29 is the sum of the five channel geometric factors.

The MAGPD proton telescope design is identical to the TIROS/NOAA SEM-2 MEPED Proton Telescope, except that the MEPED proton telescope has a thinner Al SSD coating of 20 ug/cm^2 to allow detection of protons down to 30 keV. The MEPED proton telescope is light sensitive, but on the polar-orbiting NOAA spacecraft it never views the sun, so this is not a problem. The MEPED proton telescope has five (5) differential proton energy channels and one (1) integral proton channel: 30-80 keV (0P1 and 9P1); 80-250 keV (0P2 and 9P2); 250-800 keV (0P3 and 9P3); 800-2500 keV (0P4 and 9P4); 2500-6900 keV (0P5 and 9P5); and >6900 keV (0P6 and 9P6). The MEPED proton channels should have a response identical to the MAGPD telescopes, but with different channel energies. The MEPED proton telescopes were calibrated at the GSFC accelerators. The calibration of the PM MEPED was reported in Ref. 2, and was performed according to the Test Procedure in Ref. 3. The GSFC low energy proton calibration results for 0P1 and 0P2 are given in Table 3-31, while the 9P1 and 9P2 results are in Table 3-32.

Table 3-29. Measured 1MPi and Total Geometric Factors for Protons at GSFC

Proton Energy (keV)	Gf(E) (cm2-sr)					
	1MP1	1MP2	1MP3	1MP4	1MP5	Total
69.1	7.26E-07	0	0	0	0	7.26E-07
74.2	8.06E-05	5.19E-07	0	0	0	8.12E-05
79.3	1.12E-03	4.70E-07	0	0	0	1.12E-03
85.0	4.34E-03	2.35E-07	0	0	0	4.34E-03
97.8	5.92E-03	1.46E-06	0	0	0	5.92E-03
106.9	4.71E-03	1.70E-04	0	0	0	4.88E-03
111.3	4.37E-03	2.06E-03	0	0	0	6.43E-03
116.7	6.74E-04	5.59E-03	0	0	0	6.27E-03
122.5	6.21E-05	6.13E-03	1.53E-07	0	0	6.20E-03
157	1.48E-05	1.62E-02	1.37E-05	1.22E-06	0	1.62E-02
200	6.48E-06	2.00E-05	1.84E-02	2.37E-06	6.90E-07	1.84E-02
218	6.41E-06	1.96E-05	6.31E-03	5.39E-07	2.35E-07	6.34E-03
241	8.01E-06	1.18E-05	1.27E-02	6.60E-04	1.23E-06	1.34E-02
274	5.72E-06	8.05E-06	3.63E-05	7.47E-03	1.02E-06	7.52E-03
521	1.31E-05	3.77E-05	2.22E-05	1.95E-05	8.81E-03	8.90E-03

Table 3-30. Measured 1MPi and Total Area(0 degrees) for Protons at GSFC

Electron Energy (keV)	A(0°) (cm2)					
	1ME1	1ME2	1ME3	1ME4	1ME5	Total
69.1	3.27E-05	0	0	0	0	3.27E-05
74.2	1.33E-03	0	0	0	0	1.33E-03
79.3	1.69E-02	0	0	0	0	1.69E-02
85	5.49E-02	0	0	0	0	5.49E-02
97.8	6.71E-02	3.72E-06	0	0	0	6.71E-02
106.9	5.43E-02	2.98E-03	0	0	0	5.72E-02
111.3	4.40E-02	2.65E-02	0	0	0	7.05E-02
116.7	5.73E-03	6.58E-02	0	0	0	7.15E-02
122.5	4.95E-04	7.18E-02	2.83E-06	0	0	7.23E-02
157	1.88E-04	1.96E-01	2.23E-04	1.05E-05	0	1.97E-01
167	3.39E-05	7.91E-03	1.26E-02	5.65E-06	0	2.06E-02
177	1.02E-04	1.27E-03	2.26E-01	3.96E-05	0	2.27E-01
188	4.21E-05	3.37E-04	1.60E-01	1.58E-05	0	1.61E-01
200	8.36E-05	3.06E-04	1.85E-01	6.26E-05	4.64E-06	1.86E-01
218	1.03E-04	1.89E-04	7.42E-02	1.37E-05	0	7.45E-02
241	9.28E-05	1.46E-04	1.14E-01	5.40E-03	3.39E-06	1.19E-01
253	7.63E-05	6.10E-05	2.12E-03	3.64E-02	7.63E-06	3.87E-02
264	4.36E-05	1.16E-04	1.31E-04	5.25E-02	0	5.28E-02
274	5.65E-05	1.27E-04	2.18E-04	8.12E-02	3.59E-06	8.17E-02
315	6.49E-05	7.79E-05	3.90E-05	6.17E-03	0	6.36E-03
347	1.39E-05	5.55E-05	9.72E-05	1.55E-02	2.64E-02	4.21E-02
358	1.43E-04	2.34E-04	1.04E-04	5.26E-04	6.15E-02	6.25E-02
419	2.47E-04	2.60E-05	1.30E-05	0	1.62E-04	4.48E-04
521	2.64E-04	4.97E-04	2.69E-04	2.76E-04	1.32E-01	1.33E-01
672	7.18E-05	2.99E-04	1.20E-04	1.02E-04	3.29E-02	3.35E-02
775	7.18E-05	1.98E-04	3.82E-04	1.26E-04	1.79E-01	1.80E-01
785	9.42E-05	1.47E-04	2.99E-04	1.15E-04	2.14E-01	2.15E-01
792	1.82E-05	2.73E-05	1.37E-04	3.19E-05	5.97E-04	8.11E-04
797	1.62E-05	1.62E-05	1.38E-04	2.84E-05	5.63E-04	7.62E-04
806	1.03E-05	9.27E-05	3.19E-04	7.73E-05	1.67E-04	6.67E-04

Table 3-31. PM TIROS/NOAA MEPED 0 deg Telescope Proton Calibrations at GSFC

Proton Energy (keV)	Area(0 deg) (cm**2)		Gf (cm**2-sr)	
	0P1	0P2	0P1	0P2
31	0.0671	-	0.0169	-
36	0.0896	-	0.0223	-
50	0.0951	-	0.0232	-
56	0.0759	-	0.0183	-
66	0.0935	0.00042	0.0194	0.00015
80	0.0605	0.0191	0.0142	0.00319
88	0.0109	0.0673	0.00324	0.0124
104	0.00062	0.0680	0.00021	0.0131

Table 3-32. PM TIROS/NOAA MEPED 90 deg Telescope Proton Calibrations at GSFC

Proton Energy (keV)	Area(0 deg) (cm**2)		Gf (cm**2-sr)	
	9P1	9P2	9P1	9P2
25	0.0147	-	0.00143	-
31	0.0536	-	0.00555	-
35	0.0906	-	0.00878	-
39	0.0815	-	0.00774	-
50	0.0885	-	0.00840	-
71	0.0911	0.00031	0.00840	0.00001
79	0.0665	0.0262	0.00626	0.00232
89	0.00508	0.0965	0.000548	0.00957
100	0.00052	0.0982	0.000053	0.0109

The results for the GSFC Gf(E) and A(E,0) are shown in Figures 3-5 and 3-6. The previous proton calibration data from Ref. 2 are shown in Figures 3-7 (Gf) and 3-8 (A(0)), along with the 1MP1 and 1MP2 measurements from GSFC. The present measurements are in reasonable agreement with the previous MEPED calibrations, with the proton energies shifted appropriately. The magnitude of the Gf(E) maximum value varies somewhat for different measurements, but tends to be near the calculated value of 0.0100 cm^2-sr. The MAGPD GSFC proton calibration data is slightly low at low energies, but is in better agreement with calculations at high energies. This is most likely a proton beam alignment problem, since the GSFC proton beam is sometimes quite difficult to center on the sensor being calibrated.

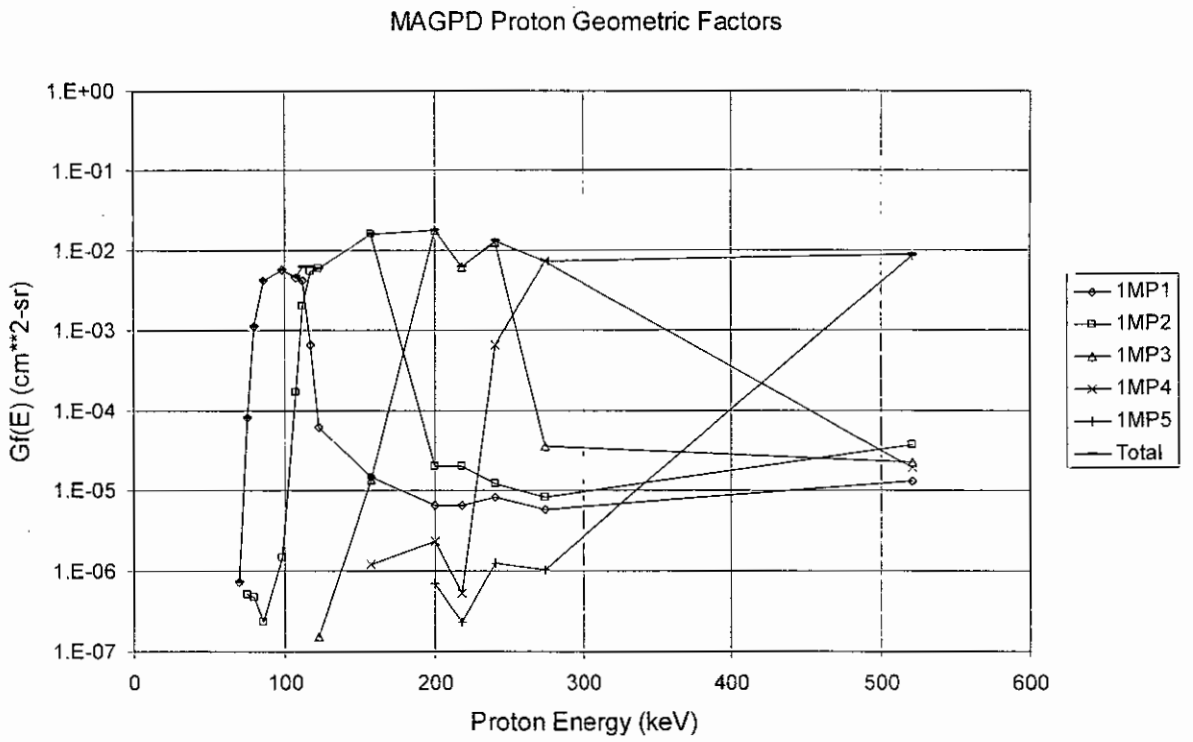

Figure 3-5. MAGPD Gf(E) Plots for GSFC Proton Calibration Data

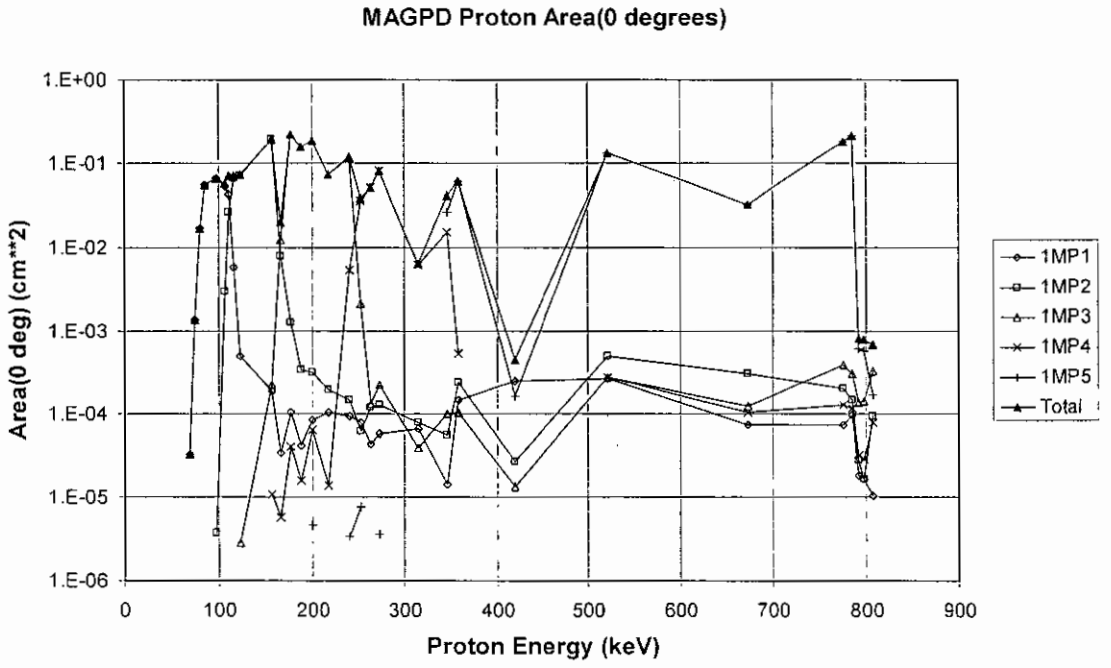

Figure 3-6. MAGPD Area(0 deg, E) Plots for GSFC Proton Calibration Data

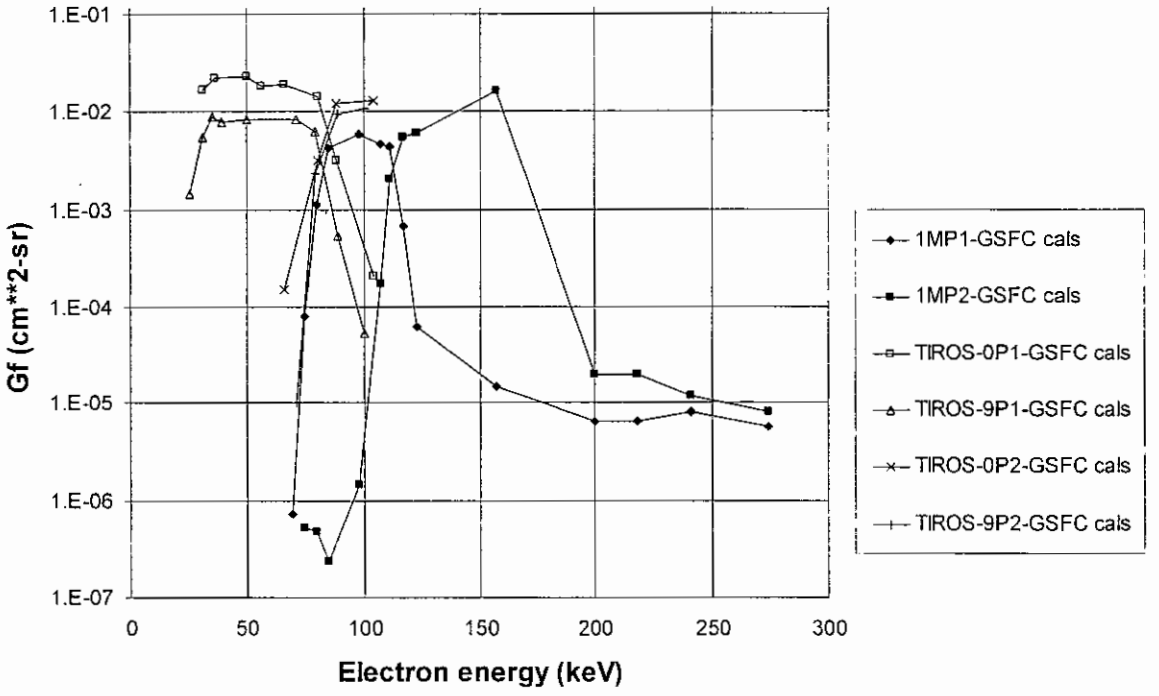

Figure 3-7. MAGPD and MEPED Gf(E) Plots for Proton Calibration Data

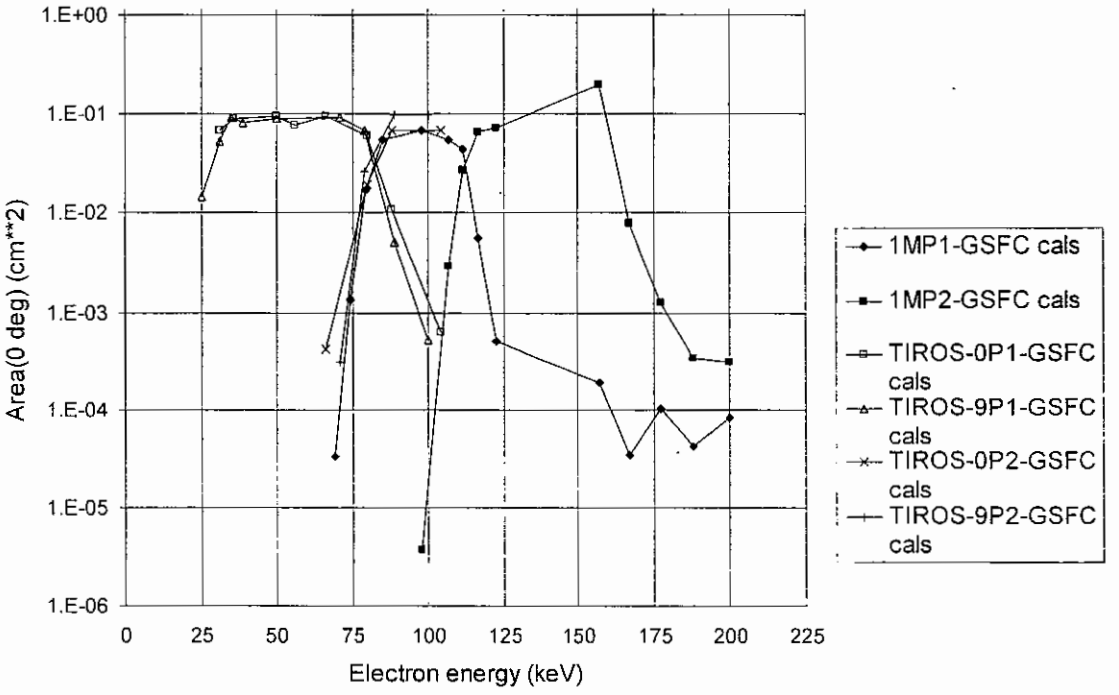

Figure 3-8. MAGPD and MEPED Area(0 deg, E) Plots for Proton Calibration Data

3.2.2 Electron Geometric Factors

The measured electron geometric factors, obtained by integrating over the angular measurements given in Tables 3-17 through 3-28, using the procedure described in Section 2.2, for all 1MPi channels, are summarized in Table 3-33. The total values in Table 3-33 are the sum of the five channel values. The results for the MIT Gf(E) are shown in Figure 3-9.

Table 3-33. Measured 1MPi and Total Geometric Factors for Electrons at MIT

Electron Energy (keV)	Gf(E) (cm2-sr)					
	1MP1	1MP2	1MP3	1MP4	1MP5	Total
770	1.23E-04	4.11E-04	1.78E-04	2.78E-04	1.59E-04	1.15E-03
802	2.06E-04	6.01E-04	1.91E-04	2.33E-04	1.47E-04	1.38E-03
1140	4.53E-04	1.16E-03	2.10E-04	2.65E-04	1.22E-04	2.20E-03
1620	1.65E-03	1.53E-03	2.13E-04	1.57E-04	6.85E-05	3.61E-03
2100	9.94E-04	1.82E-03	3.08E-04	2.19E-04	1.09E-04	3.46E-03
2600	5.64E-03	6.50E-03	3.59E-03	3.65E-03	1.43E-03	2.08E-02

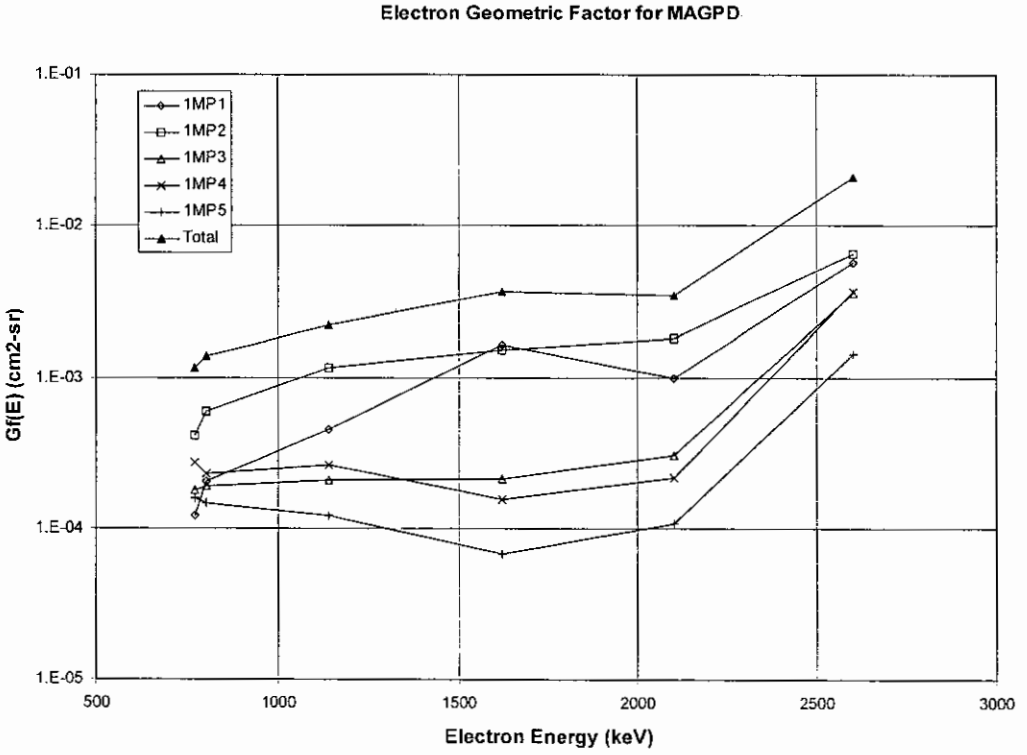

Figure 3-9. MAGPD Gf(E) Plots for MIT Electron Calibration Data

3.3 Comparison of Measured and Calculated Responses

3.2.1 Calculated Responses

The design of the MAGPD telescope is shown in Figure 2-1, and the calculated proton and electron energy losses in the front SSD are shown in Figure 3-10. The energy losses are calculated from the stopping powers given in Refs. 4 and 5 for electrons, and in Ref. 6 for protons. The calculations assume a nominal front SSD Al coating thickness of 120 ug/cm^2 and a front SSD thickness of 200 um Si. The rear SSD is also 200 um Si, and is used in anti-coincidence with the front SSD, so high energy protons are vetoed by the rear SSD. The channel energy breakpoints are listed in Table 3-34. The SSDs are shielded from low energy electrons by the magnets, and only electrons above several hundred keV can reach the front SSD. Very high energy electrons should also be vetoed by the rear SSD, since they are likely to deposit energy in both SSDs.

The calculated Area(0 degrees) = 0.0856 cm^2, and the total geometric factor is Gf = 0.0100 cm^2-sr. Proton energy deposits are expected to be reasonably accurate, since there is minimal scattering of protons in the Al and Si SSDs. At very high energies the proton energy loss drops because the dE/dx energy loss decreases and the protons penetrate the SSDs. The stopping power (dE/dx) reaches a minimum at about 2000 MeV, so the high energy proton energy loss never goes below the lower threshold for MP4. However, the rear SSD vetoes all high energy protons from all of the MPi channels.

Electrons scatter significantly, and for the highest energy electrons (>>1 MeV) there will be a significant fraction depositing the ionization energy loss value, although this will be a broad distribution in energy. Thus the MP1, MP2, and MP3 channels are expected to have a moderate high energy electron response, as shown in the MIT data in Figure 3-9.

The measured proton data are in reasonable agreement with the calculations, with the A(0 degrees) values generally being near 0.0856 cm^2 for full channel (or summed-channel) responses, and the Gf values (generally for the channel-summed values) are near 0.010 cm^2-sr. The proton calibrations are discussed in more detail in Section 3.3.2, with best-fit Gf(E) functions being provided for data analysis. The electron calibrations are discussed in more detail in Section 3.3.3, with best-fit Gf(E) functions being provided for use in correction of the proton flux data using the MAGED measurements.

Table 3-34. Calculated Proton and Electron MAGPD Channel Energies

Threshold Values and Particle Energies					Channel Logic	
Front SSD Threshold No.	Threshold Value (keV)	Low Proton Energy (keV)	High Proton Energy (MeV)	Electron Energy (keV)	MAGPD Channel	Threshold Range
Level 1	24.4	80.	-	25.4	MP1	1 to 2
Level 2	55.2	110.	-	55.8	MP2	2 to 3
Level 3	121.5	170.	358	121.9	MP3	3 to 4
Level 4	208.	250.	146	(-)	MP4	4 to 5
Level 5	314.	350.	82.5	(-)	MP5	5 to 6
Level 6	776.	800.	26.0	(-)		

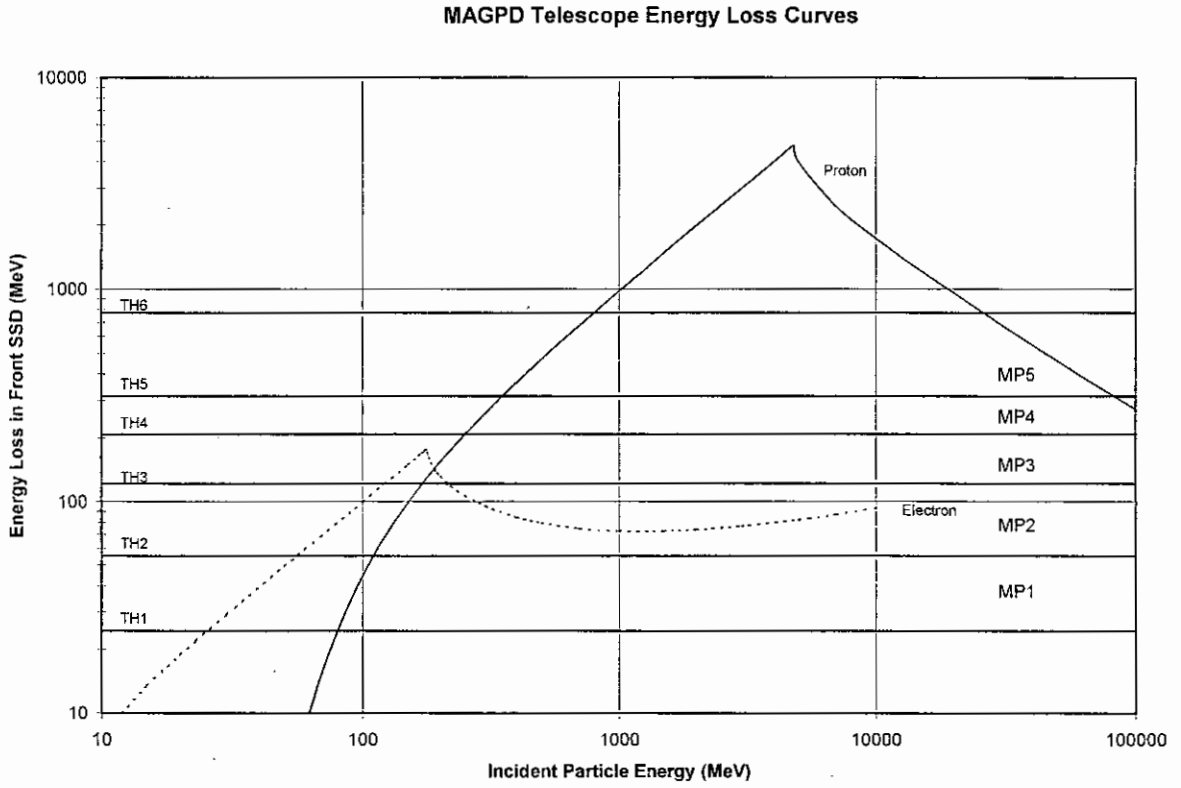

Figure 3-10. MAGPD Telescope Energy Loss Curves

3.3.2 Proton Responses

The MAGPD proton channel Gf(E) measurements are given in Table 3-29, and plotted in Figure 3-5, with additional comparisons in Figure 3-7. A better estimate of the energies where the response switches from one channel to another can be made by viewing a plot of the fractional A(0 deg), where each channel has its measured area divided by the total channel summed area. Figure 3-11 shows a plot of all of the GSFC relative measured A(0 deg) data from Table 3-30. Using these plots, the proton energies for channel switches are listed in Table 3-35, along with the calculated values from Table 3-34.

The measured electron transition energies agree well with the calculated values, with the following comments:

1. The lowest energy threshold is approximately 80 keV, taken from the rise in the 1MP1 Gf(E) data. This is in good agreement with the calculated threshold.

2. The four channel transition energies (calculated = 110, 170, 250, and 350 keV) have the measured values all within the range of +2 keV to –5 keV of the calculated value. This is good agreement with the calculated values.

3. The highest energy threshold is approximately 790 keV, taken from the fall in the 1MP5 Gf(E) and Area(0 degrees) data. This is in good agreement with the calculated threshold.

4. The low energy (<150 keV) Gf(E) values tend to be below the calculated value of 0.0100 cm^2-sr; the A(0 deg) values are closer to the calculated 0.0856 cm^2. The high energy (>150 keV) Gf(E) values tend to be above the calculated value of 0.0100 cm^2-sr; the A(0 deg) values have a moderate range in magnitude about the calculated 0.0856 cm^2. These results are from problems with proton beam alignment, as discussed in Section 3.2.1. Overall there is in good agreement with the calculated Gf(E) value.

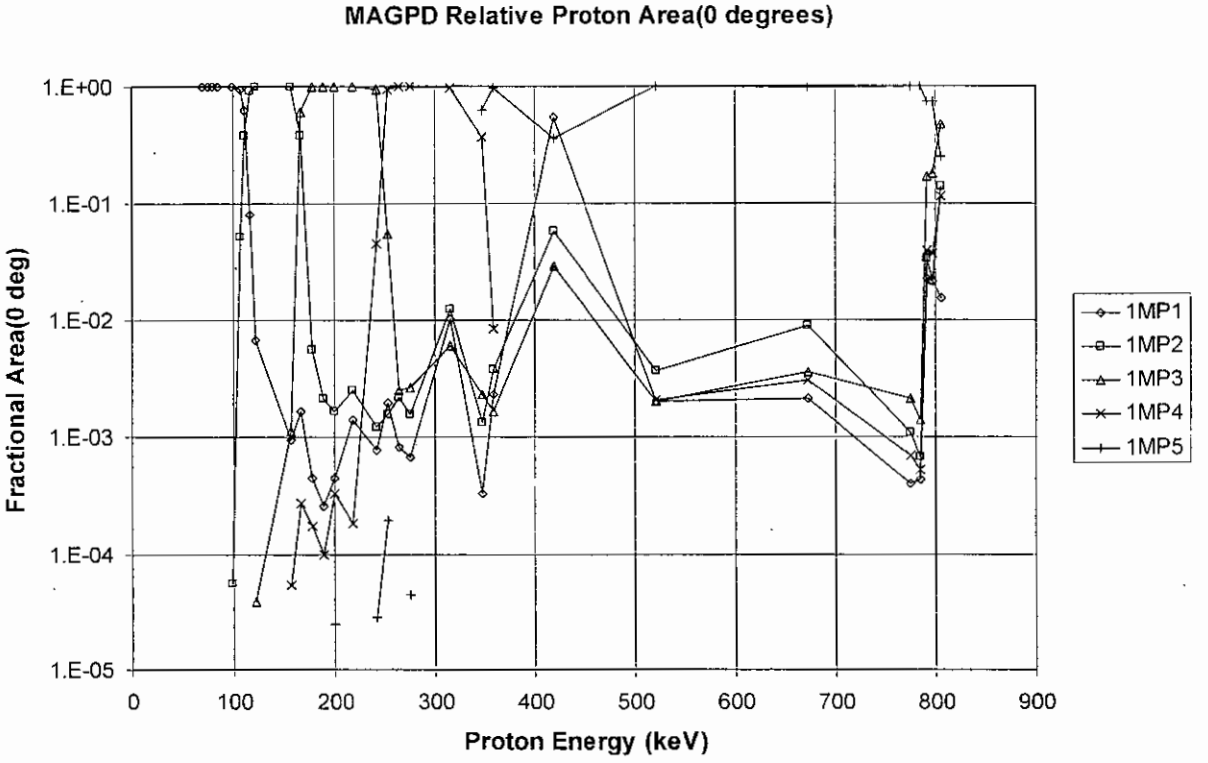

Figure 3-11. Measured Relative 1MPi A(0 deg) Values as a Function of Proton Energy

Table 3-35. Measured MAGPD Proton Channel Transition Energies

Threshold Level	Channel Transition	Transition Energies (keV)	
		Calculated	Measured
Level 1	MP1 / On	80	80
Level 2	MP1 / MP2	110	112
Level 3	MP2 / MP3	170	166
Level 4	MP3 / MP4	250	247
Level 5	MP4 / MP5	350	345
Level 6	MP5 / Off	800	790

The MAGPD proton channel measured responses are close to the calculated responses. The recommended effective proton energy-geometric factors for the MAGPD proton channels are listed in Table 3-36, and shown for each individual channel, along with the measured data, in Figures 3-12 to 3-16.

Table 3-36. Recommended MAGPD Proton Channel Gf(E) Values for Protons

MP1 Gf(E)		MP2 Gf(E)		MP3 Gf(E)		MP4 Gf(E)		MP5 Gf(E)	
Energy (keV)	Gf(E) (cm^2-sr)	Energy (keV)	Gf(E) (cm^2-sr)	Energy (keV)	Gf(E) (cm^2-sr)	Energy (keV)	Gf(E) (cm^2-sr)	Energy (keV)	Gf(E) (cm^2-sr)
75	1.0E-4	105	1.0E-4	165	1.0E-4	245	1.0E-4	345	1.0E-4
85	1.0E-2	115	1.0E-2	175	1.0E-2	255	1.0E-2	355	1.0E-2
105	1.0E-2	165	1.0E-2	245	1.0E-2	345	1.0E-2	795	1.0E-2
115	1.0E-4	175	1.0E-4	255	1.0E-4	355	1.0E-4	805	1.0E-4

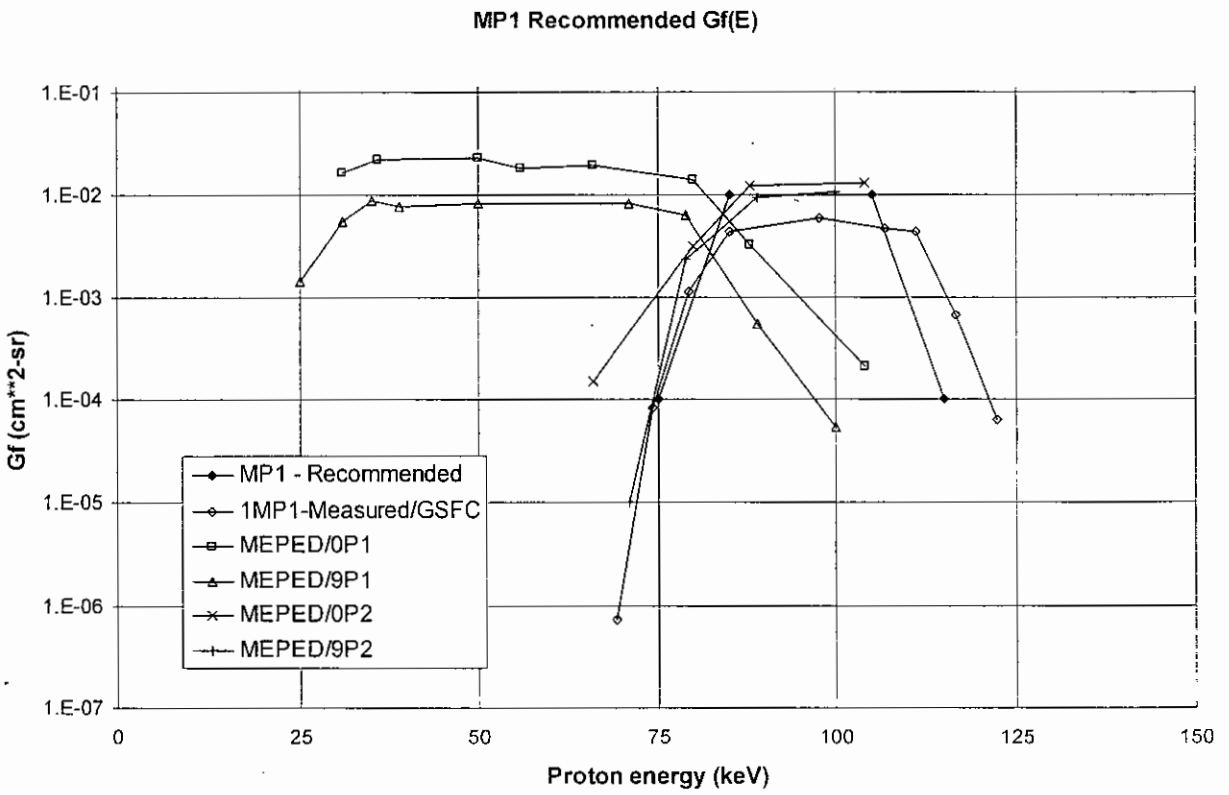

Figure 3-12. Recommended and Measured MP1 Gf(E) Values as a Function of Proton Energy

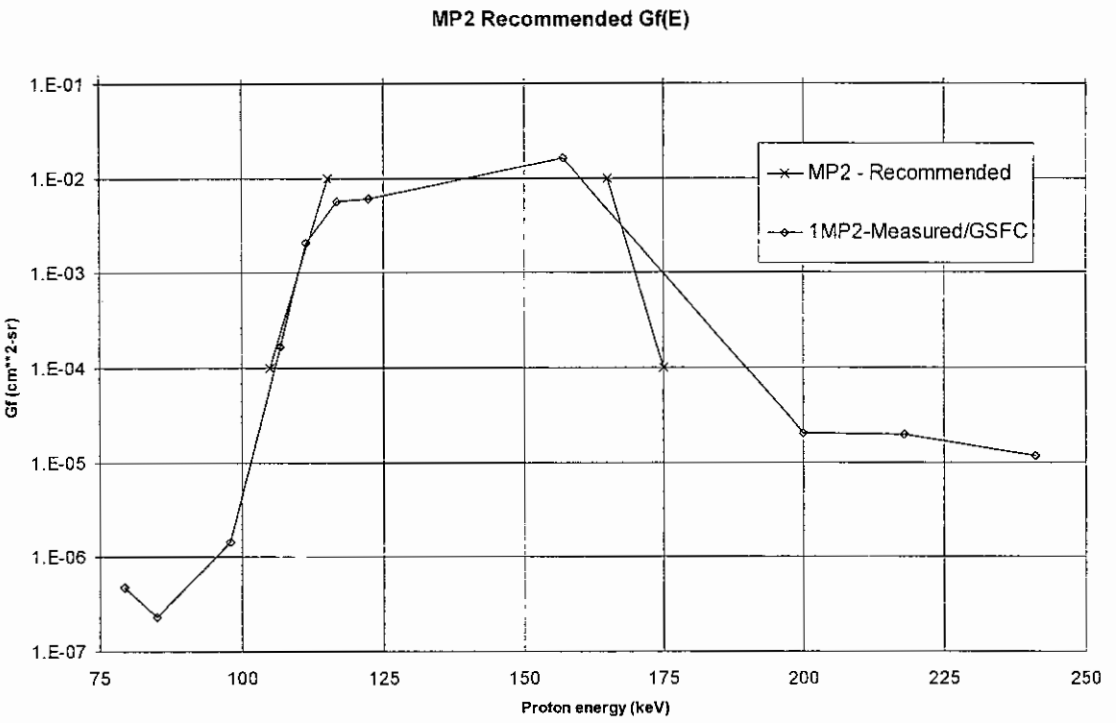

Figure 3-13. Recommended and Measured MP2 Gf(E) Values as a Function of Proton Energy

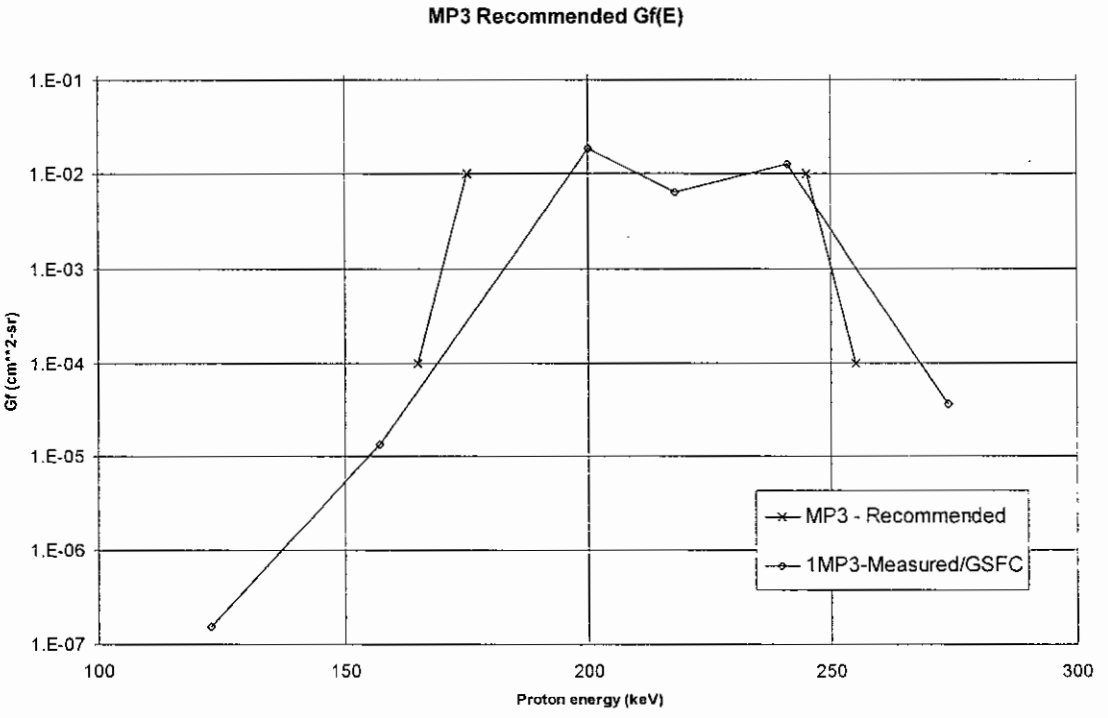

Figure 3-14. Recommended and Measured MP3 Gf(E) Values as a Function of Proton Energy

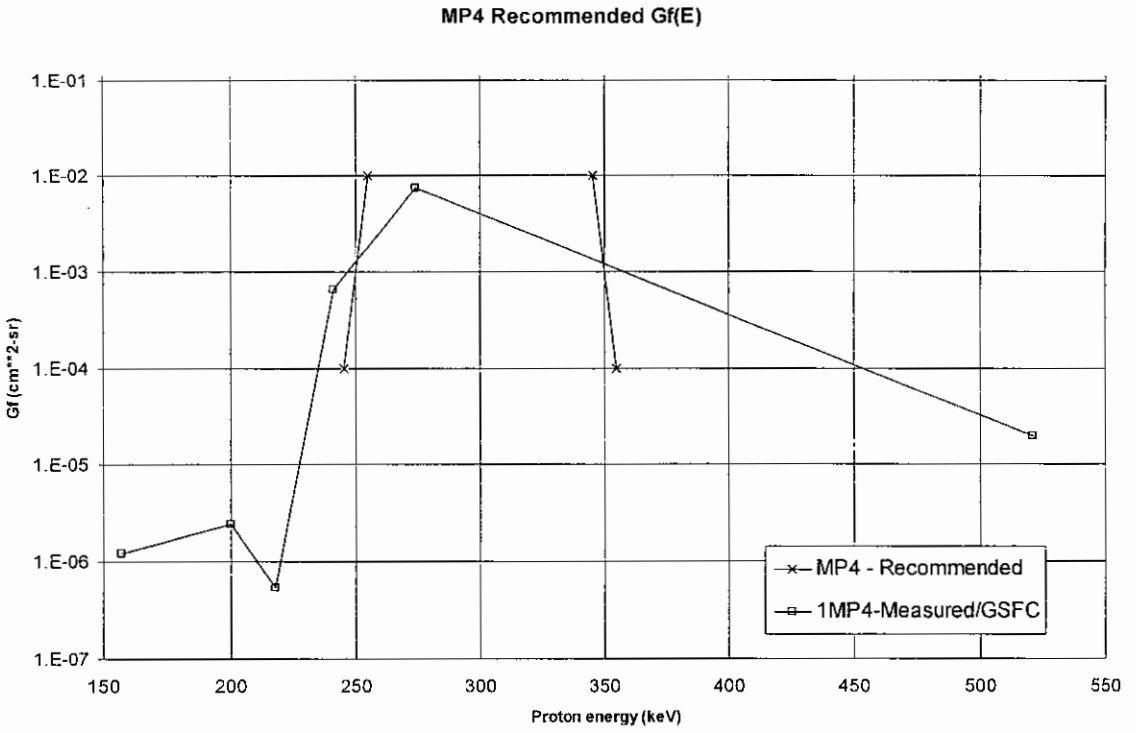

Figure 3-15. Recommended and Measured MP4 Gf(E) Values as a Function of Proton Energy

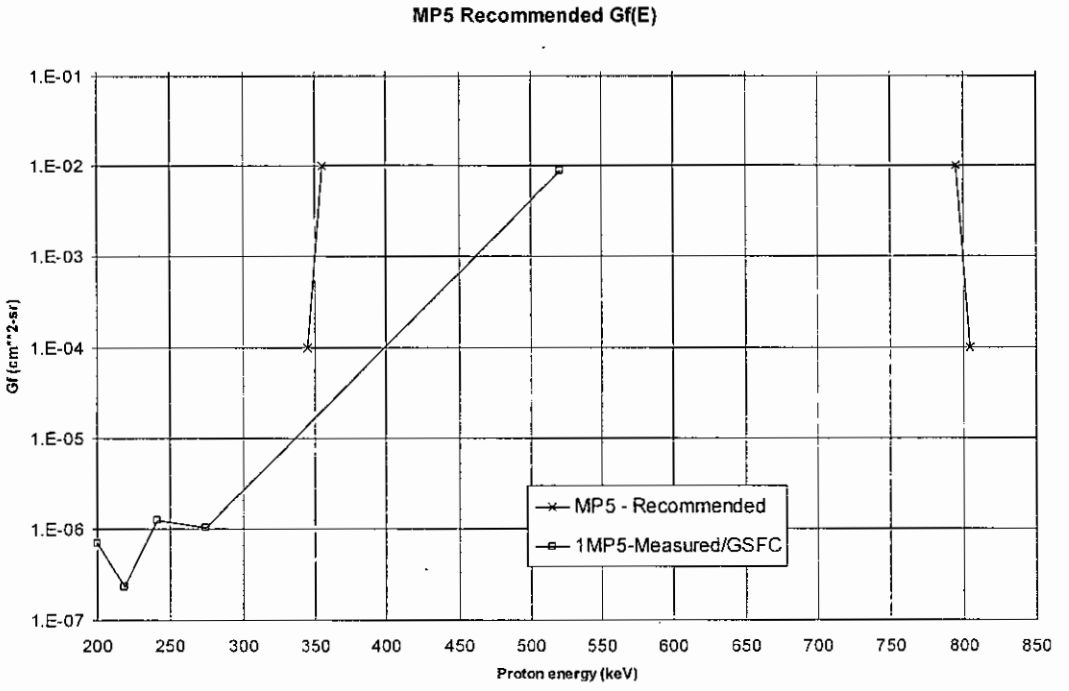

Figure 3-16. Recommended and Measured MP5 Gf(E) Values as a Function of Proton Energy

All MPi channel have a recommended response very close to the calculated response. The rise and fall edges have about a 10 KeV width, mostly from the FWHM noise of the SSD. The channel edge energies are best defined by the more detailed A(0 deg) data, especially the relative plots in Figure 3-11. The high energy Gf(E) data are too sparse to define the channel edges, but they do show agreement with the peak Gf(E) values. The high energy proton beam at the GSFC VdeG was slightly misaligned with the calibration chamber, so it was difficult to get good aslignment and angle scans at the higher energies. A few good measurements were obtained, but much of the energy band edge data comes from the relative area data.

The calibrated proton Gf(E) responses can be used to calculate proton spectra from the measured channel count rates. This involves integrating assumed spectral shapes over the Gf(E) curves, and determining the spectral parameters from the best fit to the measured data. The recommended Gf(E) values should be used, and are estimated to be accurate to +/-25%.

3.3.3 Electron Responses

The MAGPD proton channel Gf(E) measurements for electrons are given in Table 3-33, and plotted in Figure 3-9. The data in Table 3-33 provide the best values for the electron Gf(E) for the MAGPD proton channels. The dominant response is in the MP2 channel, which is were the relativistic electron dE/dx energy loss lies. The estimated accuracy of the electron responses is about +/-25%.

4.0 SUMMARY AND CONCLUSIONS

The MAGPD 1MPi proton channel responses have been calibrated with proton and electron beams at accelerators at GSFC and MIT. The results are in reasonable agreement with previous calibrations of these channels. The calibrated geometric factors can be used to reduce in-orbit count rate data to proton fluxes. The energy and angular responses are in reasonable agreement with the expected theoretical responses.